Evaluation of Flow Redistribution due to Flow Blockage in Rod Bundles Using COBRA Code Simulation

NP-1662
Research Project 1380-2

Final Report, January 1981

Prepared by

NUS CORPORATION
4 Research Place
Rockville, Maryland 20850

Principal Investigators
D. A. Prelewicz
M. A. Caruso

Prepared for

Electric Power Research Institute
3412 Hillview Avenue
Palo Alto, California 94304

EPRI Project Manager
Bill K. H. Sun

Water Reactor System Technology Program
Nuclear Power Division

ORDERING INFORMATION

Requests for copies of this report should be directed to Research Reports Center (RRC), Box 50490, Palo Alto, CA 94303, (415) 965-4081. There is no charge for reports requested by EPRI member utilities and affiliates, contributing nonmembers, U.S. utility associations, U.S. government agencies (federal, state, and local), media, and foreign organizations with which EPRI has an information exchange agreement. On request, RRC will send a catalog of EPRI reports.

NOTICE

This report was prepared by the organization(s) named below as an account of work sponsored by the Electric Power Research Institute, Inc. (EPRI). Neither EPRI, members of EPRI, the organization(s) named below, nor any person acting on their behalf: (a) makes any warranty or representation, express or implied, with respect to the accuracy, completeness, or usefulness of the information contained in this report, or that the use of any information, apparatus, method, or process disclosed in this report may not infringe privately owned rights; or (b) assumes any liabilities with respect to the use of, or for damages resulting from the use of, any information, apparatus, method, or process disclosed in this report.

Prepared by
NUS Corporation
Rockville, Maryland

EPRI PERSPECTIVE

PROJECT DESCRIPTION

The calculations made from the current PWR design evaluation models result in core flow blockage for the design-basis loss-of-coolant accidents. The flow blockage is predicted to be caused by the swelling and rupture of the fuel rods under the conservative licensing assumptions set for the calculations. To study the effect of flow blockage on the effectiveness of the emergency cooling heat transfer, EPRI has a program which includes in-house model development, 21-rod bundle and 163-rod bundle testing and analysis (RP959), and a subchannel cross-flow study (RP1378). This project, which is part of the RP1380-2 project workscope, is an effort to assist EPRI staff in the flow blockage analysis.

PROJECT OBJECTIVE

The purpose of this study is to assess the applicability of the COBRA IV code, a multichannel model, for analyzing flow redistribution in a blocked rod bundle with geometries typical of those used in the FLECHT SEASET program 21-rod bundle tests. To develop a heat transfer model for a rod bundle with flow blockage, it is essential to analyze the flow in the bundle in terms of local subchannels because the blockage causes nonuniformity of flow. That is, a blocked zone in a rod bundle acts like a higher resistance region and tends to divert the flow toward unblocked zones.

PROJECT RESULTS

The result of this study indicates the feasibility of using the COBRA code for analyzing the flow redistribution in the FLECHT SEASET program 21-rod bundle tests. It has been planned to develop a flow blockage heat transfer model in the FLECHT SEASET program using the flow information calculated from the COBRA code. The report should

be useful to those who are interested in reactor safety heat transfer analysis.

Bill K. H. Sun, Program Manager
Nuclear Power Division

ABSTRACT

During a Loss-of-Coolant Accident, fuel rod cladding may reach temperatures approaching 2200° F. At these temperatures, swelling and rupture of the cladding may occur. The resulting flow blockage will affect steam flow and heat transfer in the bundle during the period of reflooding. The COBRA-IV-I subchannel computer code was used to simulate flow redistribution due to sleeve blockages in the FLECHT-SEASET 21-rod bundle and plate blockages in the JAERI Slab Core Test Facility. Sensitivity studies were conducted to determine the effects of spacer grid and blockage interaction, sleeve shape effects, sleeve length effects, blockage magnitude and distribution, thermally induced mixing and bundle average velocity on flow redistribution. Pressure drop due to sleeve blockages was also calculated for several blockage configurations.

TABLE OF CONTENTS

LIST OF FIGURES

LIST OF TABLES

NOMENCLATURE

d	- blockage sleeve maximum inside diameter
d'	- blockage sleeve maximum outside diameter
f_t	- turbulent momentum factor
G_B	- local mass flux in blocked subchannel
G_o	- local mass flux in unblocked subchannel
G_u	- local mass flux upstream of blockage
h_B	- local heat transfer coefficient in blocked subchannel
h_o	- local heat transfer coefficient in unblocked subchannel
K_{ij}	- cross flow resistance coefficient
K_{sp}	- spacer loss coefficient
l	- crossflow path length
L/D	- length to diameter ratio of blockage sleeve
m	- exponent in single phase heat transfer correlation
N_e	- heat transfer enhancement factor due to blockage
N_E	- heat transfer environmental factor
Re	- Reynolds number
s	- width of gap between subchannels
T_{inlet}	- steam temperature at bundle inlet
β	- turbulent mixing parameter
ΔP_{Block}	- irrecoverable pressure loss due to blockage

SUMMARY

Flow redistribution due to both sleeve and plate type blockages in rod bundles has been simulated using the COBRA-IV-I subchannel computer code. Calculations have been performed for a number of sleeve blockage configurations in the FLECHT-SEASET 21-rod bundle and for a nearly complete plate blockage of two adjacent assemblies of the 2000 rod JAERI Slab Core Test Facility (SCTF).

A number of effects were studied including interaction between blockage sleeves and spacer grids, sleeve shape effects, sleeve length effects, blockage magnitude and distribution, thermally induced mixing and bundle average velocity effects. In a small bundle, spacer grids were found to result in flow redistribution comparable to that of a sleeve blockage. Therefore, it may be necessary to include spacer grids when calculating local velocity in a blocked bundle. Thermally induced mixing does not appear to have a large effect on subchannel flow except for isolated low velocity subchannels near the periphery of the bundle. In addition, flow redistribution was shown to be only weakly dependent on bundle average velocity, flow redistribution was found to be greater for a cluster blockage than for a complete bundle blockage, and the insignificant effect of blockage sleeve low strain "tails" on the axial flow at the blockage plane was confirmed.

Simulation of a nearly complete plate blockage in the JAERI SCTF showed regions of very low flow both upstream and downstream from the blockage. This type of blockage is not typical of that which has been observed in rod bundle burst tests.

In the COBRA model, fluid may flow from one subchannel to another through the gap between subchannels. In a clean bundle, ie. a bundle without spacer grids or blockages, the gap spacing does not vary with axial location in the bundle. However, in the vicinity of a blockage the gap spacing is reduced due to the shorter distances between the

(now deformed) rods. COBRA allows the user to vary the gap spacing axially. COBRA runs for blocked bundles with and without axial gap spacing variation modeled showed that the calculated bundle flow was insensitive to the inclusion of axial gap spacing variation. The calculated flow redistribution was also found to be insensitive to inclusion of the lateral momentum flux model.

1.0 INTRODUCTION

One of the design basis events which is analyzed for nuclear power reactors is the Loss-of-Coolant Accident (LOCA). Calculations for various LOCA accident sequences show that the coolant inventory may be decreased to the point where the core is no longer covered with water. Emergency Core Cooling Systems (ECCS) are installed to provide cooling water sufficient to prevent excessive fuel damage.

Pressurized water reactors have ECCS which reflood the core from the bottom with coolant injected into the cold legs or downcomer. A quench front moves slowly up the fuel rods at a rate which may be as low as one inch per second, or less. During the period of core uncovery, the rods may reach a temperature of up to 2200^{o} F. At this temperature, swelling and rupture of the rods may occur. The resulting blockage will affect steam and entrained droplet flow above the quench front. An understanding of the flow redistribution and heat transfer effects of bundle blockages is required in order to predict the consequences of a LOCA.

A number of rod burst tests have been conducted to determine the nature and extent of fuel rod geometric changes during a LOCA. Two of these programs are the Oak Ridge National Laboratory Multi-Rod Burst Test Program[1] and the Karlsruhe Tests[2,3]. These tests indicate that the deformation will be localized near the rod peak power location.

Flow redistribution effects due to rod bundle blockages have been studied by Rowe, et al.,[4] who conducted tests of both sleeve and plate type blockages in a simple four subchannel apparatus. A sleeve type blockage is a smooth and gradual change in flow area, whereas a plate blockage is an abrupt orifice-like restriction. Rowe conducted tests with water flow at Reynolds numbers of around 10^{5} and with flow area reductions of up to 90%. Comparisons of the data and COBRA-IIIC

subchannel analysis code calculations[5] were found to be excellent.

Creer[6,7,8], et al. conducted tests with sleeve blockages in a 7 x 7 rod bundle. Tests were run with both air and water. In both cases, the COBRA code adequately predicted the velocity data near the blockages. Therefore, the COBRA subchannel code appears to be suitable for the analysis of single phase flow in the vicinity of rod bundle blockages. During reflood the flow in the bundle will consist of superheated steam with entrained droplets. Assuming that the droplets will not significantly affect the steam flow, COBRA can be used to predict local steam velocity in the vicinity of a flow blockage in a rod bundle.

Test programs are now being conducted to obtain data on the heat transfer effects of rod bundle blockages. One major effort is the FLECHT-SEASET program[9] where reflood tests with various blockage configurations will be conducted in 21-rod and 161-rod electrically heated bundles. Reflood tests with flow blockages will also be conducted in the JAERI 2000 rod Slab Core Test Facility (SCTF). Interpretation and analysis of the heat transfer data from these blockage tests will require a knowledge of the local flow conditions within the blocked bundle.

In the FLECHT-SEASET program, local flow variations due to blockages will be considered in the determination of heat transfer downstream of blockages[10]. The COBRA-IV-I program[11] will be used to calculate the local subchannel flow.

The COBRA-IV-I computer program is an extended version of the COBRA-IIIC[5] subchannel analysis code that computes flow and enthalpy distributions in nuclear fuel rod bundles and cores for both steady state and transient conditions. In addition to the capability for treating blocked channel conditions contained in prior COBRA versions, COBRA-IV-I includes: 1) the ability to model superheated steam flow; 2) the ability to treat reverse flow; and, 3) an optional pressure drop boundary condition. For a complete discussion of the code capabilities, the interested reader is referred to References 12 and 13.

In this report, steam flow redistribution due to various blockage configurations has been studied analytically using the COBRA-IV-I code. Both sleeve and plate blockages are considered. These studies consider the interaction between blockage sleeves and spacer grids, sleeve shape effects, sleeve length effects, blockage magnitude and distribution, thermally induced mixing, and bundle average velocity effects. Pressure drop due to bundle blockage has also been studied using COBRA code calculations. A method similar to that of Mincey[14] is used to predict the irrecoverable pressure drop due to several sleeve blockage configurations in the FLECHT-SEASET 21-rod bundle. This method considers the entire pressure loss to be due to area reduction. No form loss factor is included. Rowe[4] found that the area reduction loss is dominant for sleeve type blockages.

Two sleeve shapes will be tested in the FLECHT-SEASET 21-rod bundle. A short-concentric sleeve approximately 2.3 inches long has been chosen to represent the blockage shape for beta phase burst which occurs at temperatures greater than 970° C. A long non-concentric sleeve approximately 7.48 inches long will represent the alpha and mixed alpha and beta phase burst which occurs at temperatures less than 970° C. COBRA calculations were performed to determine flow redistribution for both sleeve shapes.

During the early design of the JAERI 2000 rod SCTF, consideration was given to blocking two adjacent 16 x 16 assemblies, using near 100% plate blockages. COBRA calculations were performed for this case to show the very large and non-typical flow redistribution.

2.0 FLOW BYPASS CALCULATIONS WITH SLEEVE BLOCKAGES (FLECHT-SEASET 21-ROD BUNDLE)

The FLECHT-SEASET 21-rod bundle has a heated length of 144 inches and is enclosed in a circular cross-section housing 2.69 inches in diameter. Electrically heated fuel rod simulators, 0.374 inches in diameter are placed in a square array with 0.496 inch pitch. A complete description of the test apparatus is given in Reference 10.

A series of reflood heat transfer tests will be run with various sleeve blockage configurations. Two sleeve shapes will be used to form both coplanar and noncoplanar blockages with varying amounts of flow area reduction. One objective is to determine which configuration provides the least favorable heat transfer characteristics. In order to extend the results to larger bundles and to nuclear reactor cores, it is necessary to develop an understanding of the thermal-hydraulic aspects of flow blockages, and to provide an analytical framework for calculating the effects of blockages. The heat transfer coefficient downstream of a blocked rod (h_B) is to be related to the heat transfer in the unblocked case by the relationship,

$$h_B = h_O \left[\frac{G_B}{G_O} \right]^m N_e \qquad (2.1)$$

where G_B and G_O are the local mass flux in the blocked and unblocked cases, h_O is the unblocked heat transfer coefficient, m is a parameter from a single-phase correlation, and N_e is an enhancement factor which accounts for blockage effects such as droplet breakup, increased local turbulence and blockage related vapor-droplet slip. For the case of non-coplanar blockages an additional environmental factor, N_E is to be used to account for the effects of neighboring blockages. G_B/G_O is to be calculated using the COBRA-IV-I subchannel analysis program. As discussed in Section 1.0, the COBRA-IV-I computer code is an appropriate tool for this task. Hochreiter, et al., [10, 16] have performed COBRA-IV-I calculations for various blockage sleeve geometries.

COBRA-IV-I models have been set up for the 21-rod unblocked bundle and for the same bundle with several types of blockage configurations. Two basic models have been developed, a five channel model of an octant of the bundle and an eighteen channel half bundle model. Bundle cross sections with subchannels for each COBRA model are shown in Figures 2-1 and 2-2. The octant model is used to simulate the unblocked bundle and blockages with octant symmetry. The half bundle model is used for blockages with half bundle symmetry. Geometric parameters for the octant model are given in Table 2-1.

Two different axial nodings were used in the COBRA studies. The entire 144 inch heated length was represented in one model. In the other, a thirty inch axial length in the vicinity of the blockage was modeled. Both models have sixty axial nodes. The latter model was used for the blockage studies since it allows for fine detail in the vicinity of the blockage without unnecessary calculations for many small nodes extending over the entire bundle length. COBRA-IV-I does not give the option of varying the axial node size over the bundle length.

Single egg crate spacer grids are located along the bundle length as shown in Figure 2-3. These grid spacers are treated in the model by specifying a loss coefficient at each spacer location. Loss coefficients for the spacers were assumed to have a constant value of 0.6. This value was estimated based on Rehme's [14] data.

The base model was set up for isothermal steady-state flow of superheated steam at 40 psia and 300^{o} F. Bundle average inlet velocity is taken as 31 feet/second, a value typical of reflood conditions. The Reynolds number for this situation is approximately 13,000 in the center of the bundle.

Numerical values for cross flow resistance coefficient (K_{ij}), transverse momentum parameter (s/l), turbulent momentum factor (f_t), turbulent mixing parameter (β) and the bare rod friction factor correlation coefficients were selected on the basis of the discussion in Reference 7, where COBRA modeling of air flow in a blocked bundle is considered. Table 2-2 lists basic COBRA input parameters together with the values used in the base case model.

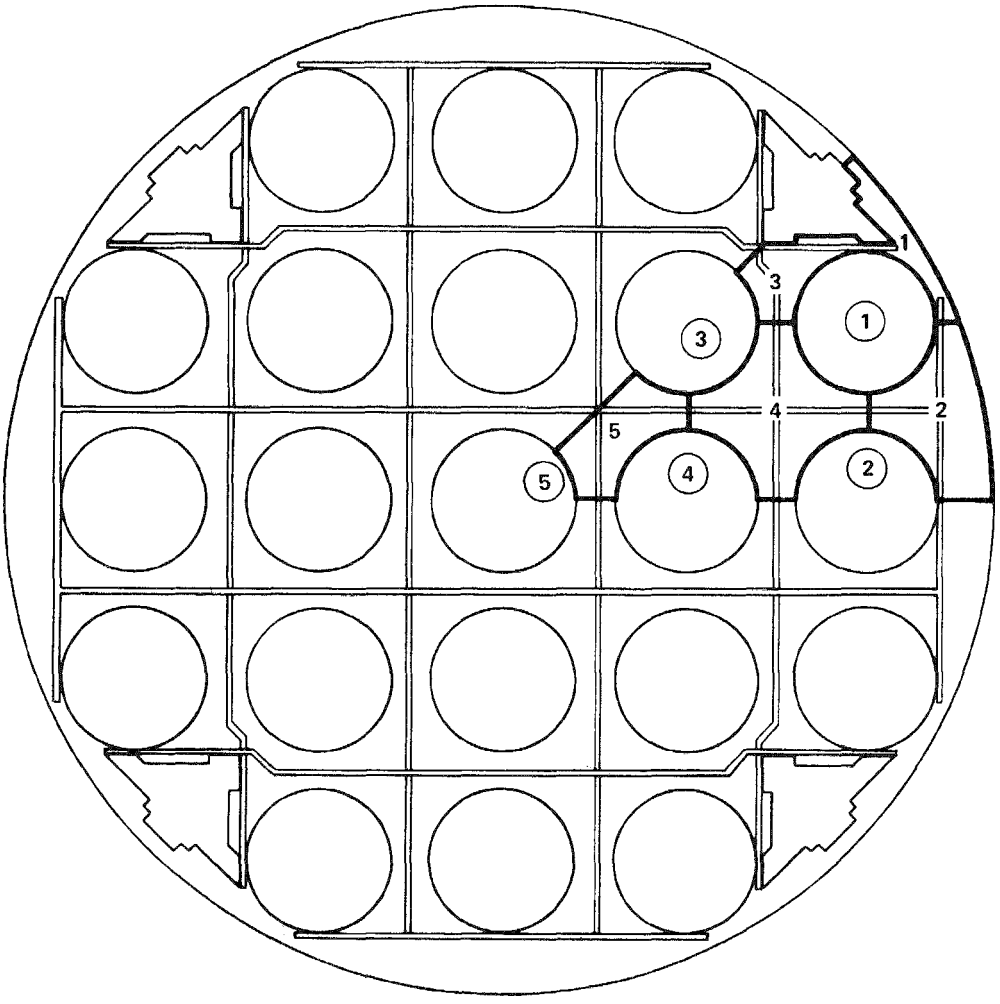

Figure 2-1

Octant Model of FLECHT-SEASET 21-Rod Bundle

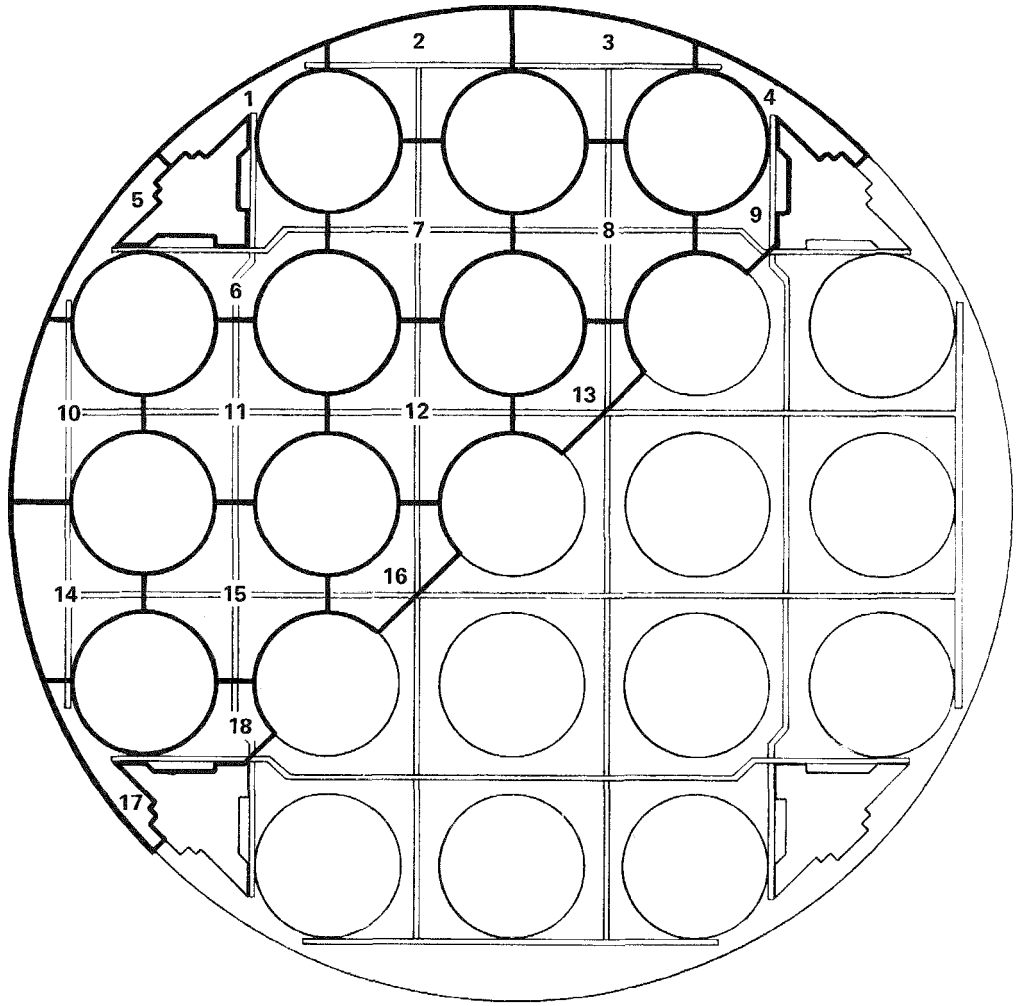

Figure 2-2

Half Bundle Model of FLECHT-SEASET 21-Rod Bundle

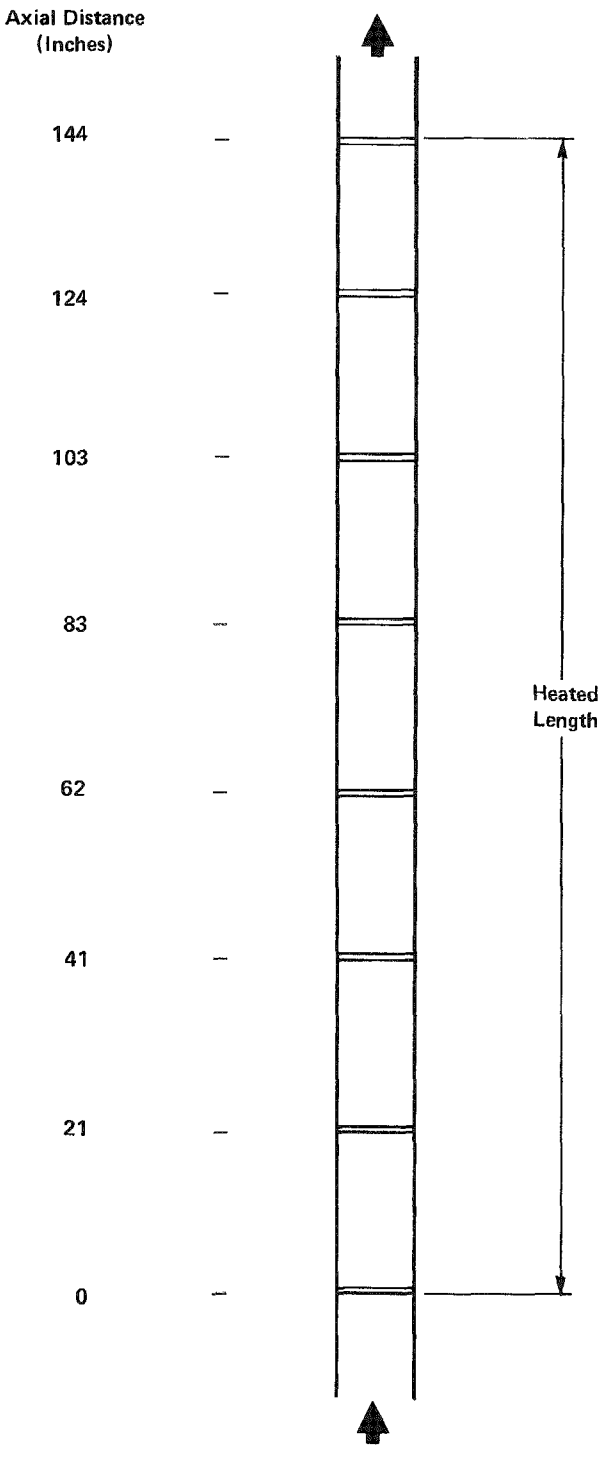

Figure 2-3

Locations of Grid Spacers in FLECHT-SEASET 21-Rod Bundle

TABLE 2-1

Subchannel Geometry Data for
Octant Model

Channel Identification[1] No.	Channel Area (Sq. In.)	Heated Perimeter (In.)	Wetted Perimeter (In.)	Hydraulic Diameter (In.)
1	0.0385	0.2937	1.187	0.1297
2	0.1039	0.5875	1.096	0.3792
3	0.0386	0.4406	0.7556	0.2043
4	0.1362	1.1750	1.175	0.4637
5	0.0681	0.5875	0.5875	0.4637

(1) Refer to Figure 2-1.

Parameters for the half-bundle model can be deduced from the above information.

TABLE 2-2

COBRA Input Parameters

Parameters	Units	Value
Steam Pressure	psia	40
Steam Temperature	^{o}F	300
Bundle Average Inlet Mass Velocity	10^6 lbm/hr-ft^2	0.01
Bundle Average Heat Flux	10^6 Btu/hr-ft^2	0.0
Cross Flow Resistance (K_{ij})	--	0.0
Transverse Momentum Parameter (s/l)	--	0.25
Turbulent Momentum Factor (f_t)	--	1.0
Friction Factor Correlation	--	$.34\ Re^{-0.25}$
Spacer Loss Coefficient (K_{sp})	--	0.6
Turbulent Mixing Parameter (β)	--	0.02

Sleeve blockages were modeled as local reductions in subchannel flow area. An additional form loss was not included. Rowe [4] and Mincey [14] have shown that for sleeve blockages reasonably accurate COBRA calculations can be performed without including this additional pressure loss.

2.1 Sleeve Length Effects

Ballooning of fuel rod cladding is quite sensitive to the local temperature distribution. This tends to localize the significant deformation in the vicinity of the peak temperature location. However, small strains may extend along the rod for many diameters. During the design stages of the FLECHT-SEASET program, the necessity of including these low strain "tails" on the sleeve was considered.

Calculations were performed [16] for sleeves with various length to diameter (L/D) ratios to determine the flow redistribution effects of sleeve length. Independently, a confirmatory analysis was performed for sleeves with three different length-to-diameter ratios.

The basic sleeve is shown in Figure 2-4. This sleeve is 2.29 inches long with an inside diameter of 0.376 inches. The maximum outside diameter is equal to the rod pitch of 0.496 inches. The central portion is cosine shaped while the end portions have a linear shape. This configuration is referred to as the short-concentric sleeve. It has an L/D of approximately six.

Three other sleeves were considered, an intermediate sleeve with L/D = 18 and two long sleeves with L/D = 37.5 and 50, respectively. The central cosine shaped portion of all the sleeves is identical. The added length is on the linear portion at each end.

COBRA simulations were performed with the octant model for the case of a single sleeve on the central rod. Spacer grids were not modeled so that redistribution effects due to blockage sleeves could be isolated. A thirty inch axial section of the bundle was modeled with the sleeve located near the center of this length. Normalized flow in the blocked subchannel (No. 5, see Figure 2-1) adjacent to the central rod is shown in Figure 2-5 for the short blockage sleeve. The flow

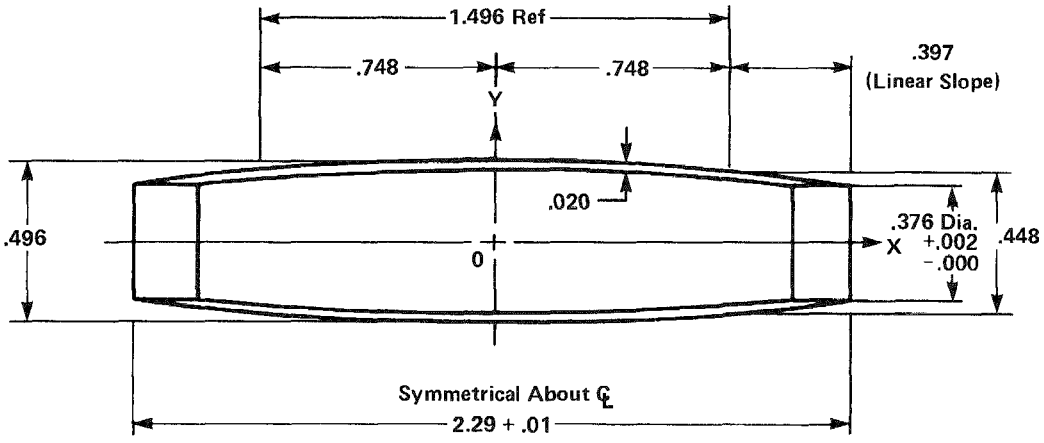

NOTE: All Dimensions Are Inches

Figure 2-4

FLECHT-SEASET Short Concentric Blockage Sleeve

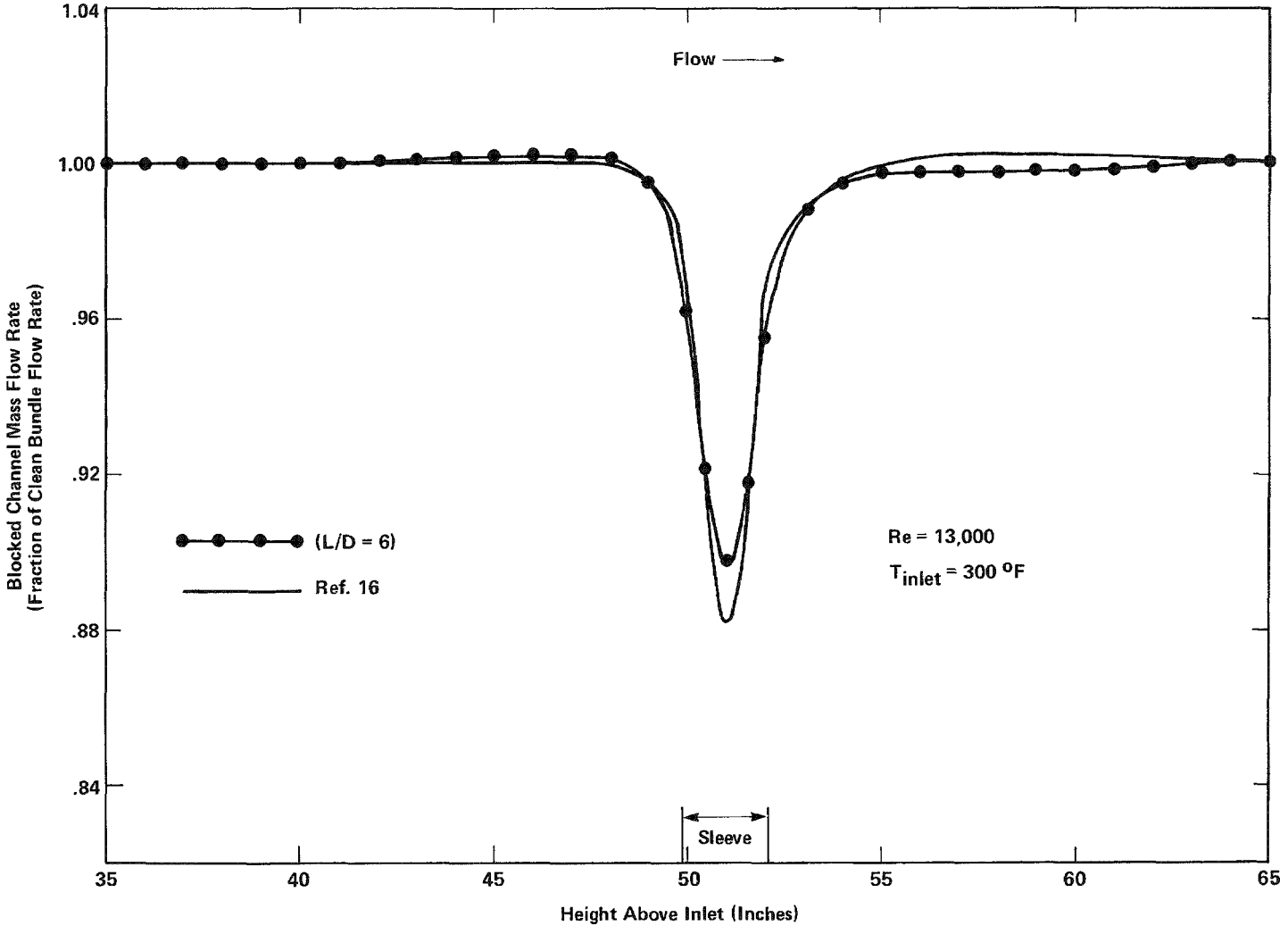

Figure 2-5

Blocked Channel Flow Rate - Short Sleeve

redistribution is localized near the blockage sleeve. Results compare reasonably well with those of Reference 16.

Flow in the blocked channel, normalized relative to the "clean"* bundle flow in the same channel, is shown in Figure 2-6 for the intermediate sleeve. Again, the results compare favorable with those of Reference 16, in terms of axial flow rate in the blockage plane. However, no flow rate increase exceeding the clean bundle flow rate was calculated to occur downstream of the blockage plane. As shown in the figure, such a "flow overshoot" had been calculated in Reference 16. Later calculations [10] did not show this behavior. The calculations presented here were instrumental in identifying this anomalous behavior in the preliminary calculations of Reference 16.

Figure 2-7 shows the axial flow rate in the blocked channel for the two long sleeves. There is only a very slight difference in this flow rate at the maximum blockage location. Therefore, flow at the plane of maximum blockage is insensitive to the length of the low strain "tail." Flow upstream and downstream is, however, affected by the presence of these low strain regions. The anomalous flow overshoot downstream of the blockage is also present in this case in the Reference 16 results.

2.2 Sleeve Shape Effects

Two types of blockage sleeves are to be used in the FLECHT-SEASET program; a short concentric sleeve (Figure 2-4) to represent Zircaloy beta phase blockage and a long non-concentric sleeve (Figure 2-8) to represent Zircaloy alpha phase blockage. Flow redistribution due to a single long non-concentric sleeve was simulated using the half-bundle model of the 21 rod bundle. The maximum strain side of the sleeve was assumed to be located on the central rod, facing a subchannel as shown in Figure 2-9. The sleeve cannot directly face a neighboring rod without mechanical interference.

*A "clean" bundle has no spacer grids and no blockages.

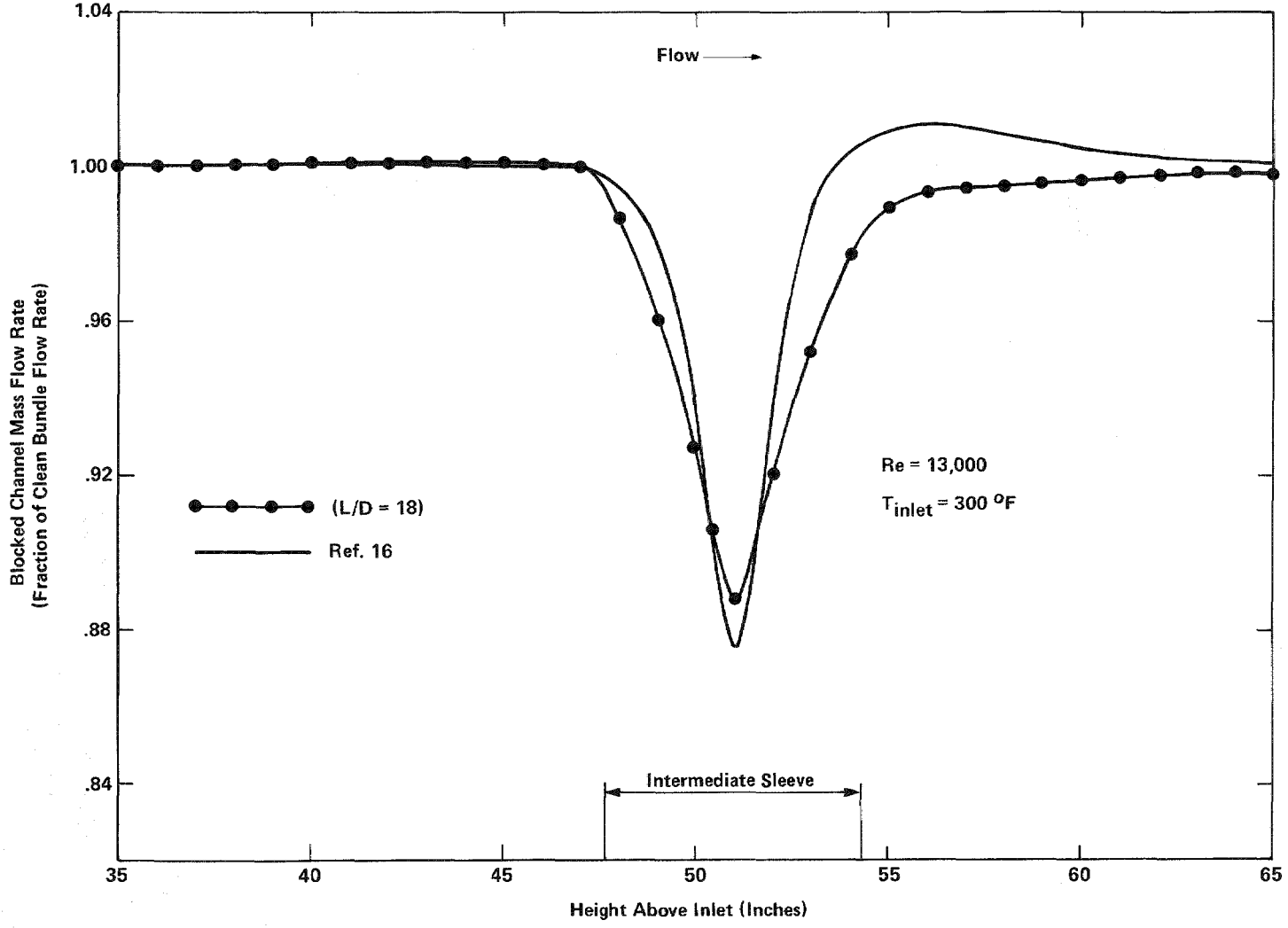

Figure 2-6

Blocked Channel Flow Rate - Intermediate Sleeve

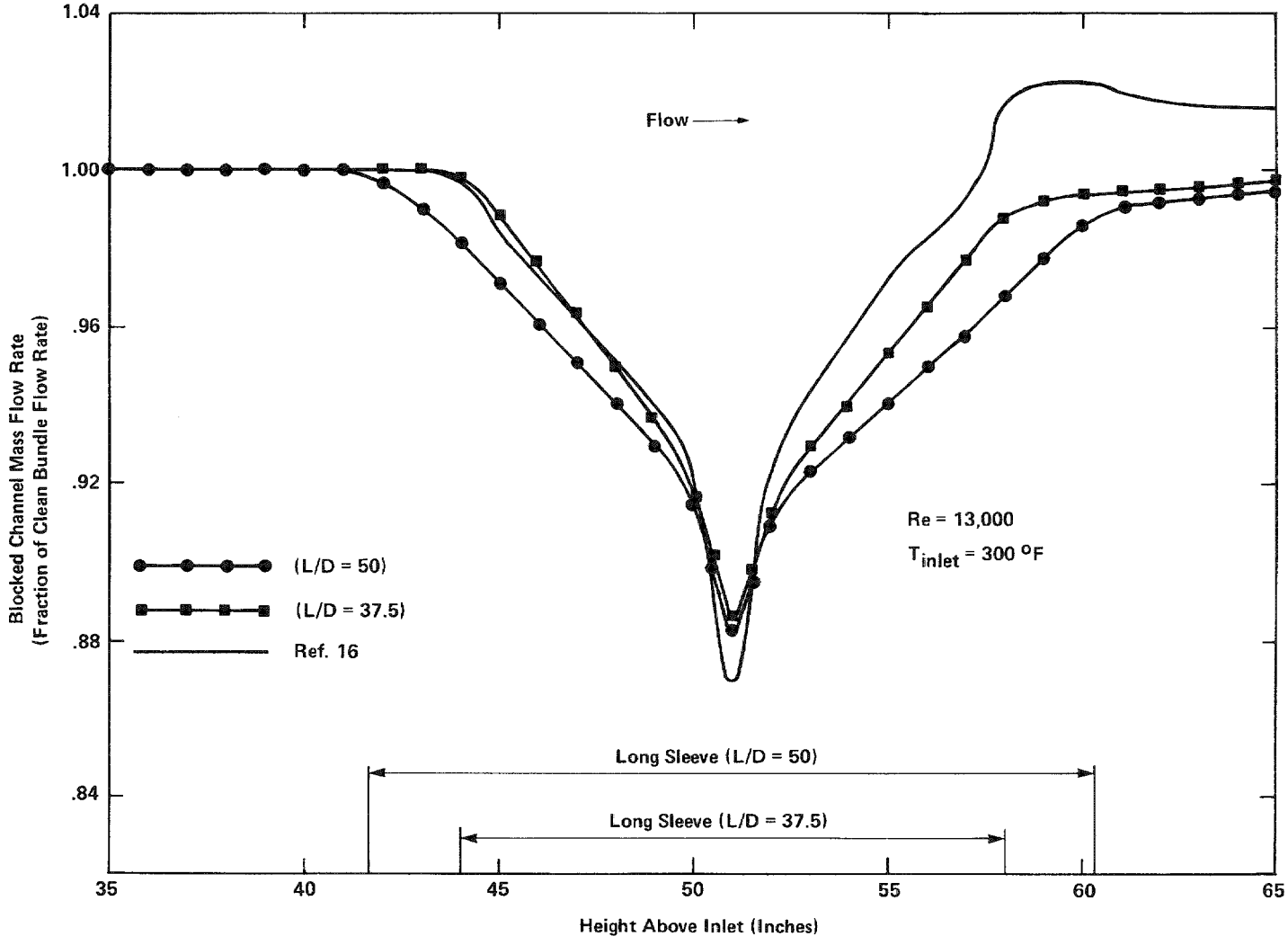

Figure 2-7

Blocked Channel Flow Rate — Long Sleeves

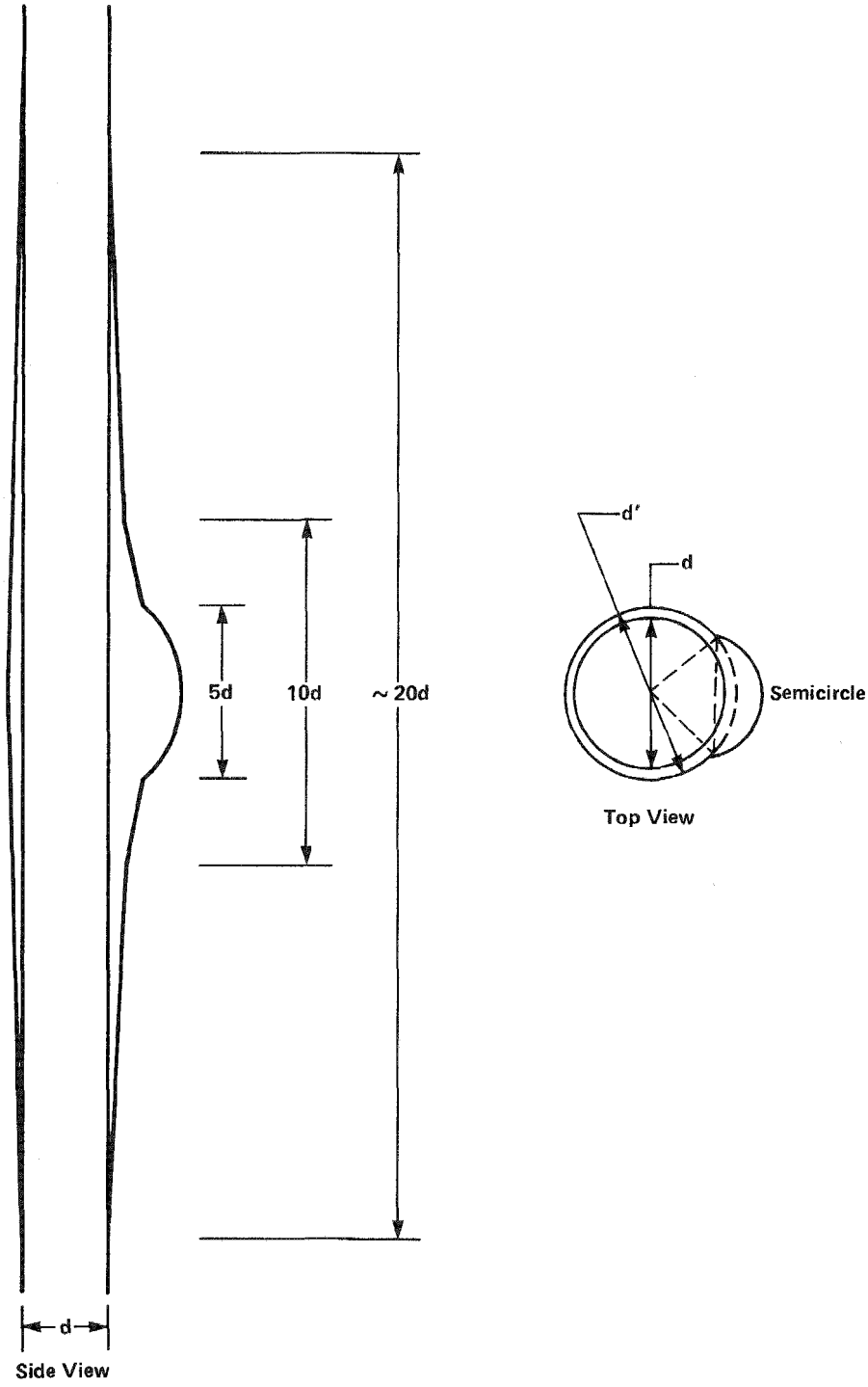

Figure 2-8

Sketch of FLECHT-SEASET Long Nonconcentric Blockage Sleeve

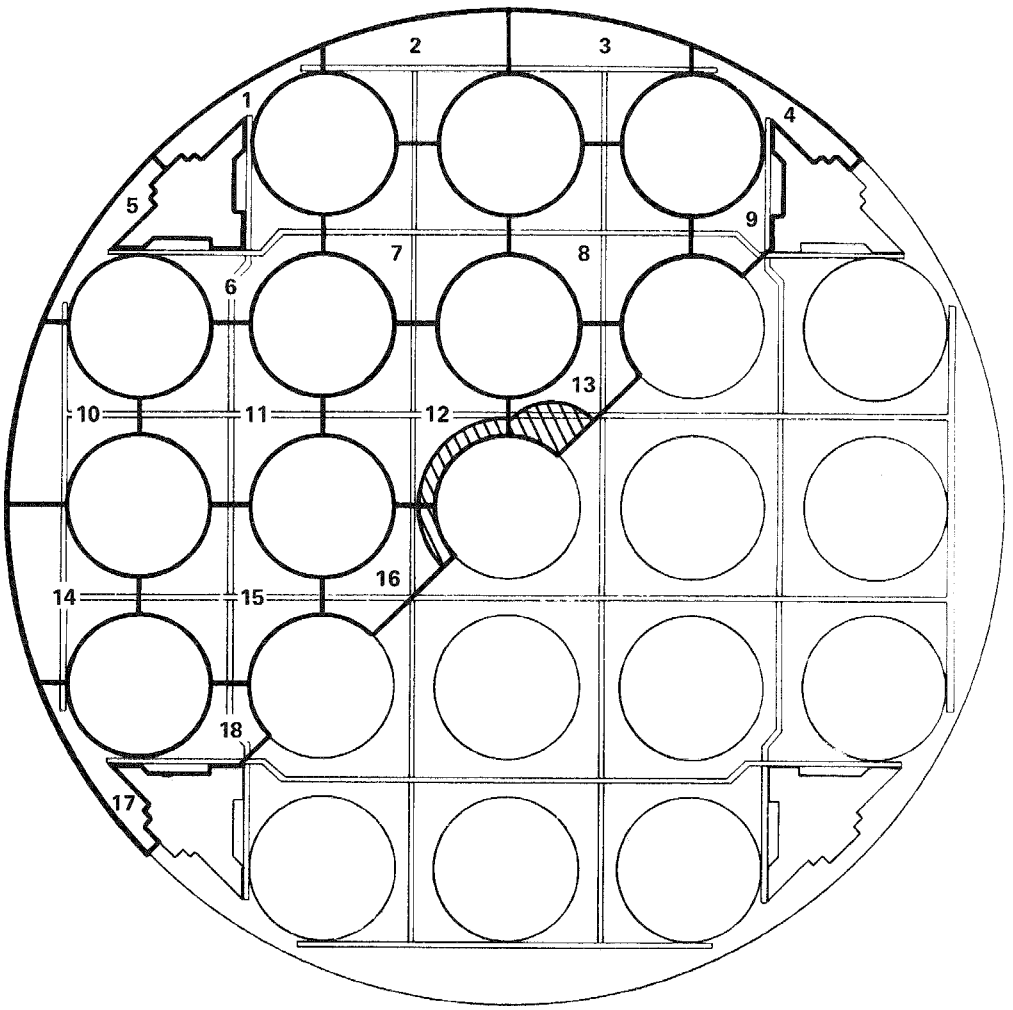

Figure 2-9

Long Nonconcentric Sleeve Blockage in the FLECHT-SEASET 21-Rod Bundle

Results of the COBRA calculations for this sleeve and the single short concentric sleeve are shown in Figure 2-10. Note that there is considerably more flow diversion for the long sleeve than there is for the short sleeve. Also, the diversion is greater on the maximum strain side (subchannel 13) than it is on the minimum strain side (subchannel 16). Hence, in analyzing data using the method embodied in equation (2.1), it may be necessary to calculate a separate h_B for each subchannel surrounding a blocked rod. It is also possible that the enchancement factor will be different for each subchannel.

2.3 Effects of Coplanar Blockage Magnitude and Distribution

The test matrix for the 21 rod bundle includes cases with: 1) a single short concentric sleeve on the center rod; 2) five coplanar short concentric sleeves on five central rods; and, 3) coplanar short concentric sleeves on all rods. Calculations of flow redistribution have been performed for these three cases using the octant model without spacer grids represented. Normalized blocked channel flows (subchannel number 5) for the three cases are shown in Figure 2-11. Note that the largest redistribution occurs for the five rod blockage configuration, since there is a larger open area near the bundle periphery. Redistribution to the outer subchannels also occurs when all rods are blocked since the outer subchannels have a smaller percentage of blocked flow area. The least redistribution occurs with the single blocked rod. Flow recovery after the blockage is slower for the larger blockages. These results show that the blockage distribution within the bundle will have a significant effect on flow diversion. The largest reduction in subchannel flow will not necessarily occur when the blockage is uniformly distributed over the bundle cross section. Rather, there will be cases where localized blockage, e.g., five rods blocked at the center of the bundle, results in greater flow redistribution.

The calculations for these cases demonstrate that COBRA is capable of simulating flow redistribution with large bypass and blockages on all rods. In performing the calculations for the case with all of the rods blocked, a numerical problem was encountered with COBRA. The problem was traced to the calculation of large cross flow resistances at the

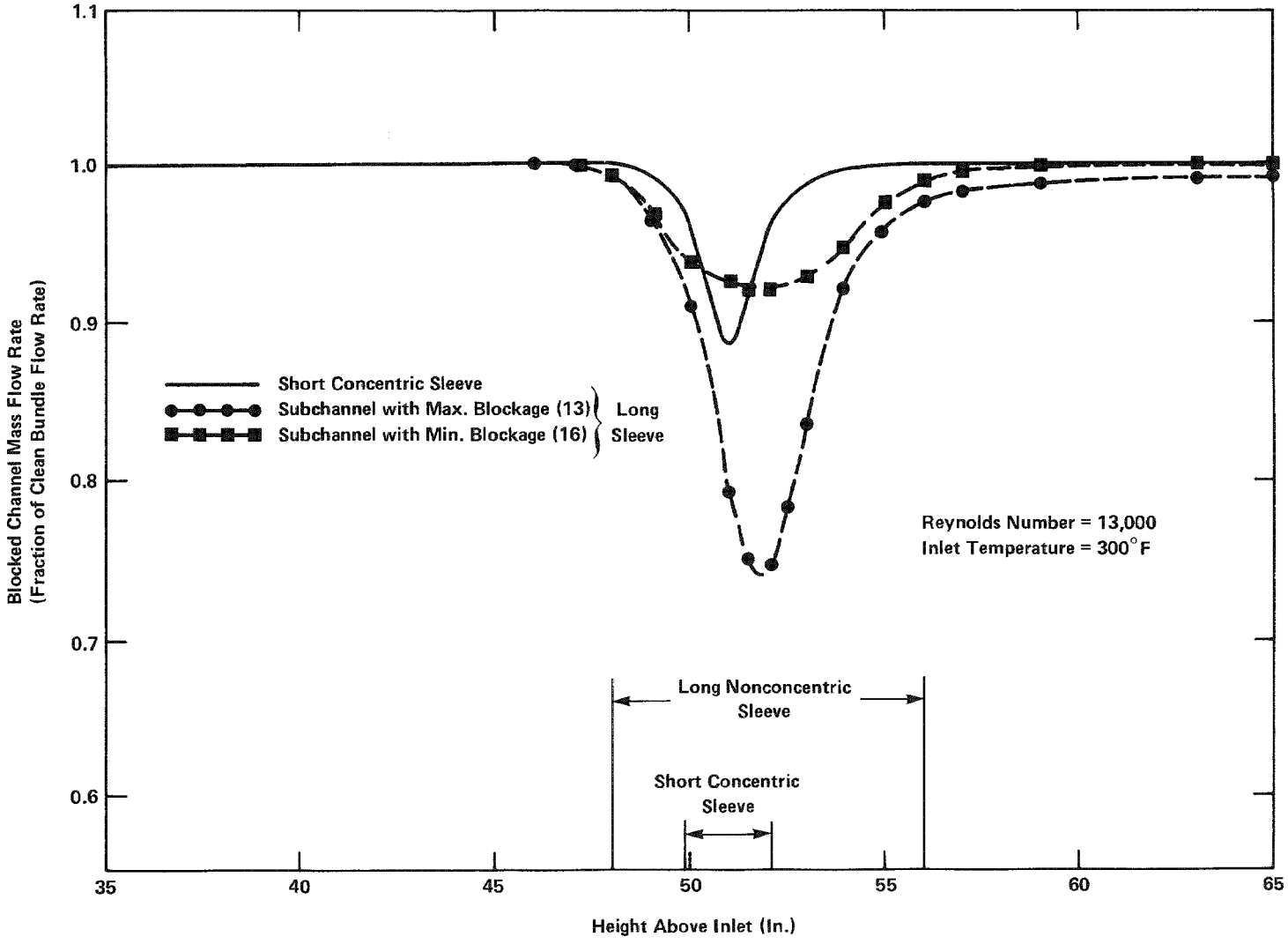

Figure 2-10

Blocked Channel Flow Rate-Long Nonconcentric Sleeve

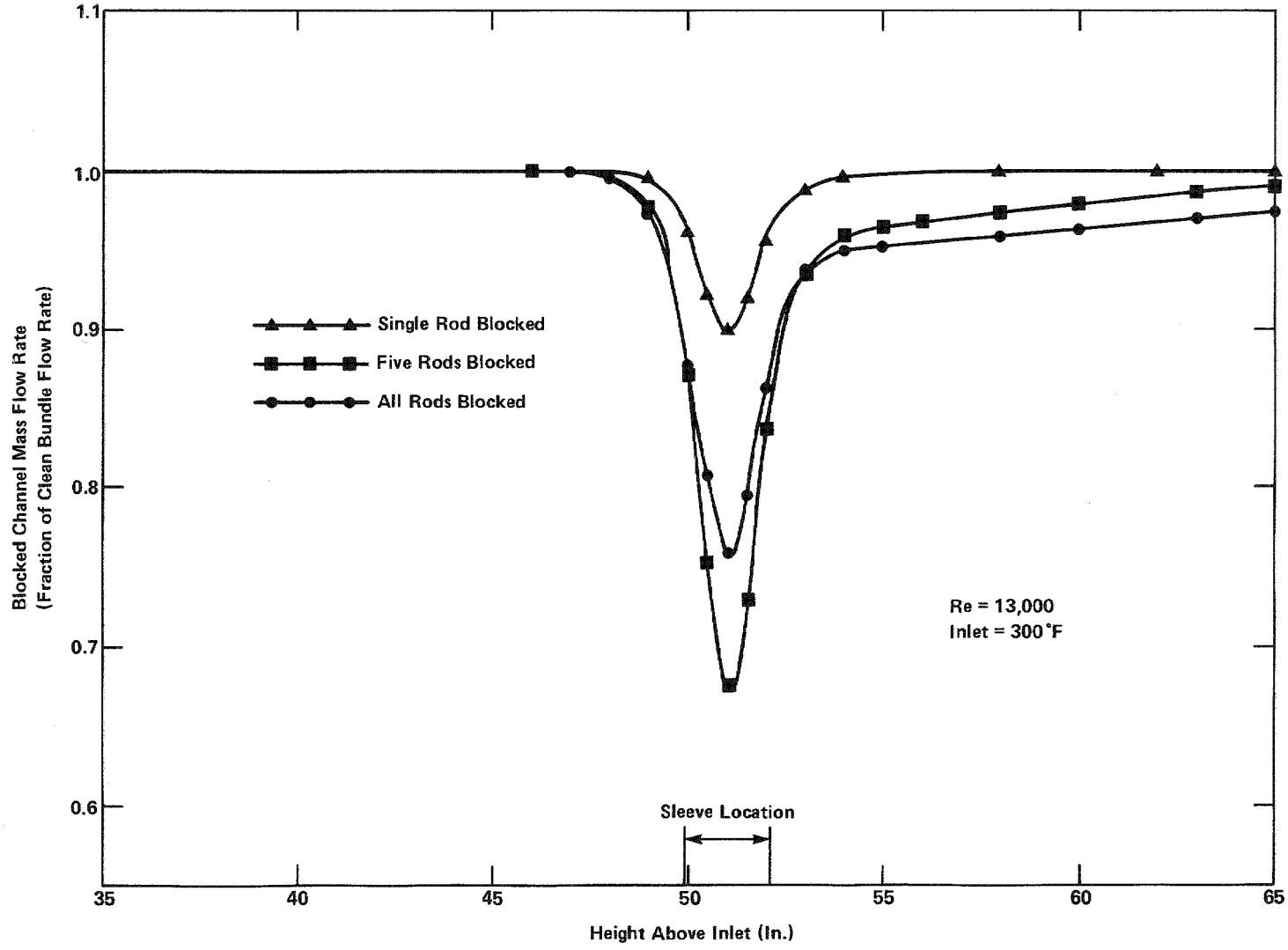

Figure 2-11

Blocked Channel Flow Rates—Multi-Rod Coplanar Blockages

maximum blockage plane. The COBRA model assumes that crossflow resistance is inversely proportional to the square of the gap spacing. At the maximum blockage plane, the gap spacing is very close to zero. A reasonable solution was obtained with COBRA, however, when the gap spacing variation model was not used.

To verify that the results are not sensitive to this input, the five blocked channel case was run both with and without variable gap spacing. The difference in the axial flows between the two cases was not greater than 0.25 percent. This result is consistent with other observations that the results are not sensitive to the cross flow resistance coefficient (Reference 12) and gap spacing variation (Reference 4). Therefore, it does not appear to be necessary to specify the gap variation to obtain valid results.

Also, the lateral momentum flux option was found to cause numerical difficulties in obtaining converged solutions. This observation is consistent with Reference 13, where it is observed that this option may cause instability in the solution for two dimensional slab geometries. Reference 13 also recommends that "...its (lateral momentum flux) effects should be evaluated carefully against experimental data before it is used." The single short concentric sleeve blockage model was run with and without this option, and no significant differences in results were obtained. This indicates that the option contributes little to the accuracy of the simulation.

2.4 Spacer Grid Effects in Small Bundles

In the 21 rod bundle, the hydraulic resistances vary widely between the interior channels and the channels which bound the filler pieces at the periphery. This is due to the increased ratio of wetted perimeter to flow area (i.e., smaller hydraulic diameter) in the peripheral channels. The fully developed velocity distribution calculated by COBRA for the clean bundle is shown in Table 2-3. The presence of a spacer grid in a subchannel produces a local resistance to flow which is proportional to the square of the flow rate. Unequal resistances at the spacer elevations due to the unequal flow rates in the subchannels and the close proximity of the interior channels to the channels near the filler lead to cross flow toward the filler

TABLE 2-3

Clean Bundle Mass Velocity Distribution

Channel Number*	Channel Inlet Mass Velocity (Fraction of Bundle Average)	(10^6 lbm/hr-ft^2)
1	0.57	0.0057
2	1.0	0.0101
3	0.80	0.008
4	1.10	0.0110
5	1.15	0.0115

* Refer to Figure 2-1 for channel locations.

piece upstream of the spacer elevations. A cross flow reversal occurs downstream of the spacer. Figure 2-12 shows the effect of these periodic changes in cross flow on the subchannel axial flow profiles.

Figure 2-13 shows the cross flow for the same case. Notice that the flow upstream of the spacer is out of Channels 4 and 5 and into Channels 3 and 1. Also notice that the flow is through Channel 2, in the sense that the flow through the gap between Channels 4 and 2 is about equal to the flow in the gap between Channels 2 and 1. Hence, there is very little change in the mass flux in Channel 2. The spacer grid perturbation is due to the unequal velocity in the subchannels. In a large bundle, this effect will be reduced significantly due to the smaller differences in subchannel flow. Therefore, this flow redistribution, which is significant when compared to the blockage flow redistribution, is unique to small bundles. Figure 2-14 snows the effect of including grid spacer pressure losses in the blocked channel calculation for the single short concentric sleeve blockage on the central rod. Normalized flow in the blocked channel is shown. Note the magnitude of the flow redistribution caused by the spacer relative to that caused by the blockage.

Since the calculated magnitude of the spacer induced cross flow is sensitive to the spacer loss coefficient, a study was performed in which the spacer loss coefficient (K_{sp}) was varied between 0.0 and 2.0. The results of this study are presented in Figure 2-15 in the form of the central subchannel (subchannel number 5 of Figure 2-1) percentage flow decrease at the spacers and at the blockage sleeve center for the various assumed spacer loss coefficients. The flow redistribution at a spacer grid location is seen to increase with increasing spacer loss coefficient, as would be expected. There is also a slight interaction between the blockage redistribution and the spacer redistribution since the blockage redistribution decreases slightly with increasing spacer loss coefficient.

The spacer grid effect will be present whenever there are high resistance channels near the periphery of the bundle. For the 21-rod bundle there is a significant impact on the center subchannel flow profile. The design criteria for the 21-rod bundle (i.e., sizing the

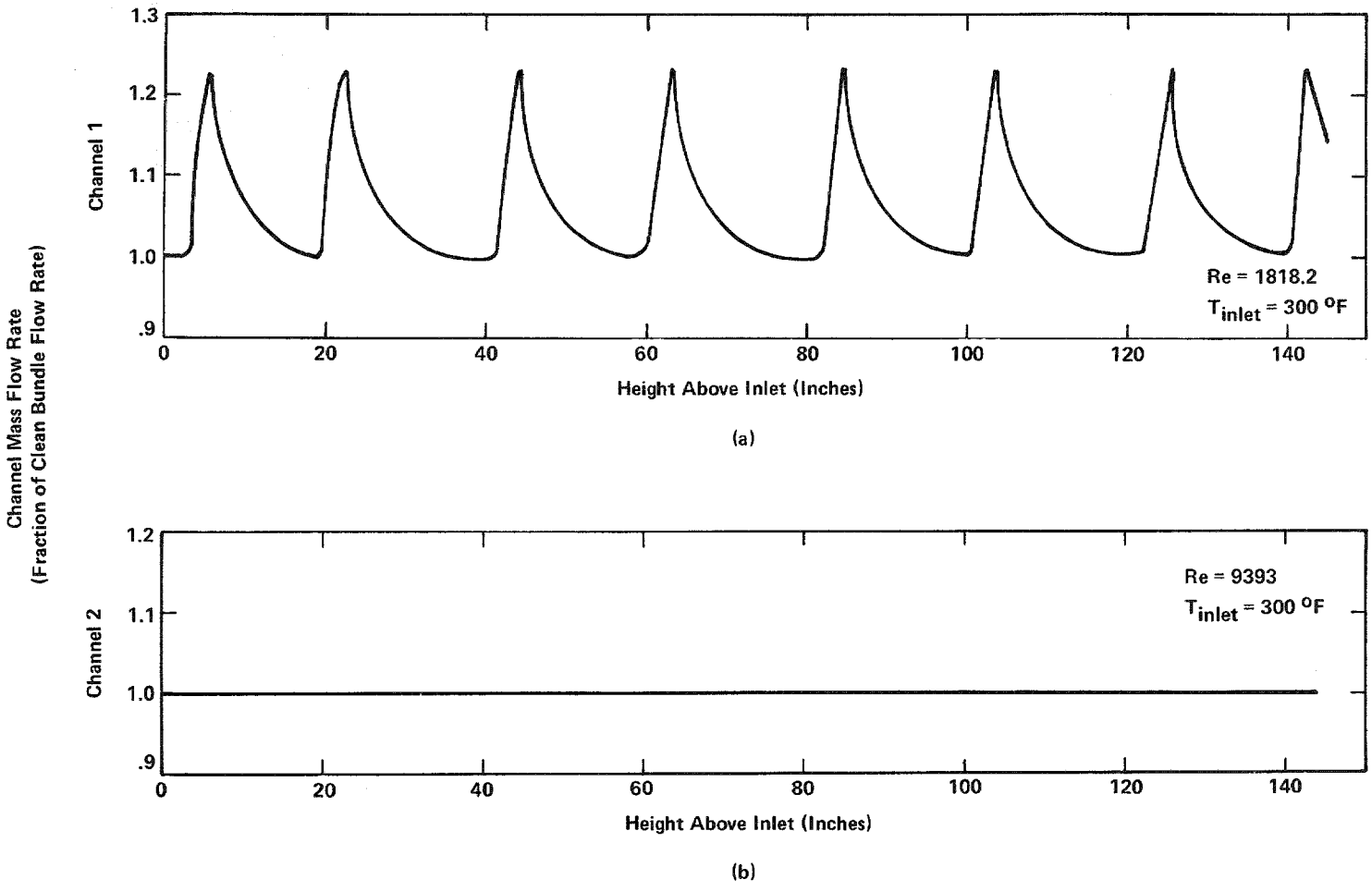

Figure 2-12

Unblocked Bundle Channel Flow Profiles

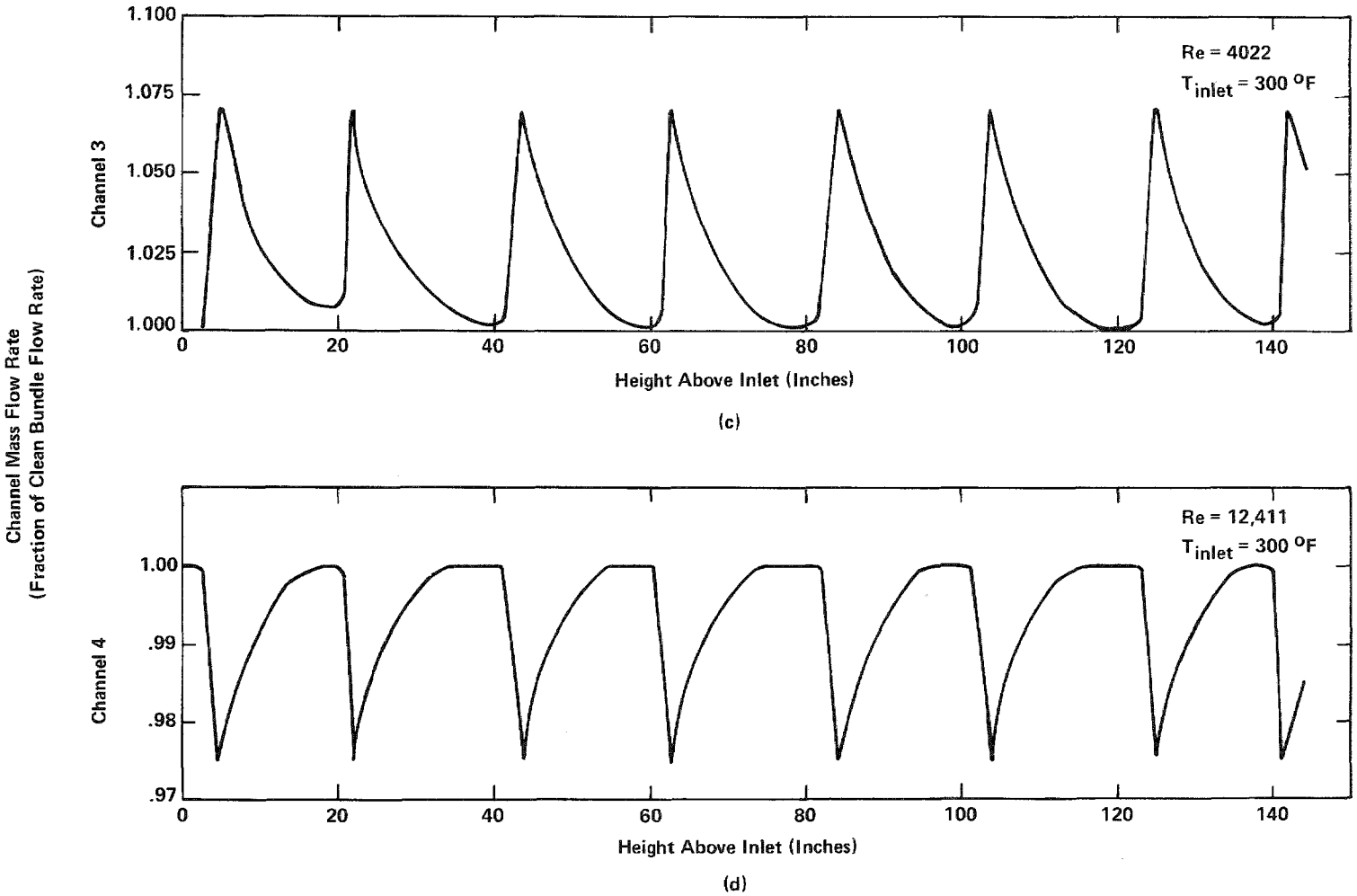

Figure 2-12

Unblocked Bundle Channel Flow Profiles (Cont.)

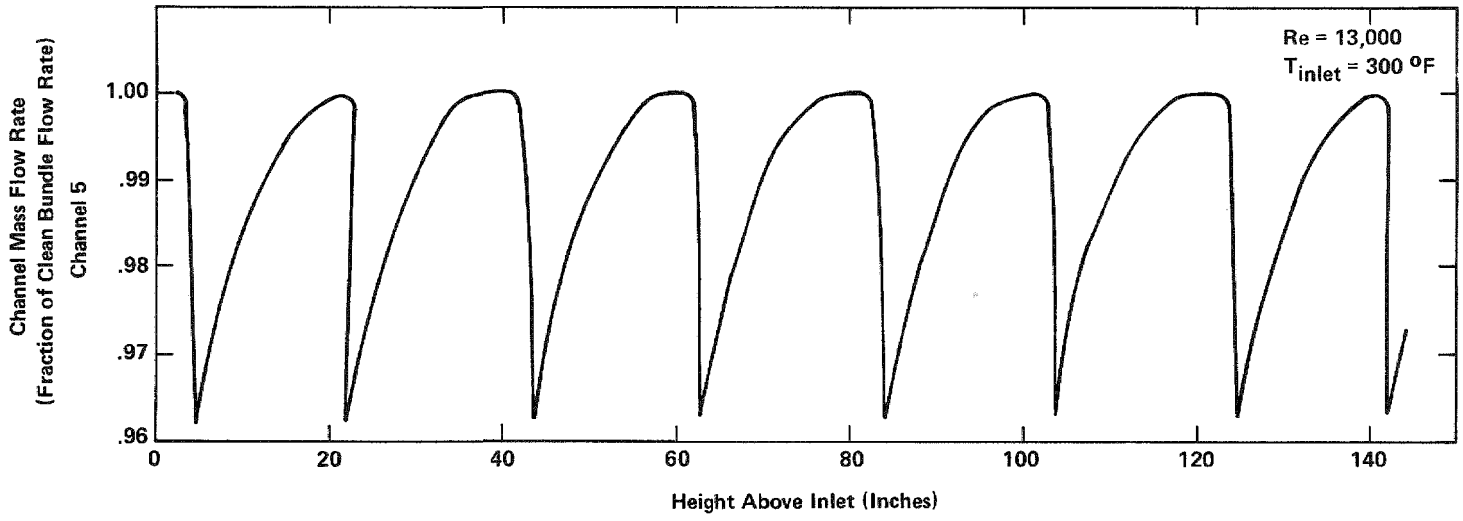

(e)

Figure 2-12

Unblocked Bundle Channel Flow Profiles (Cont.)

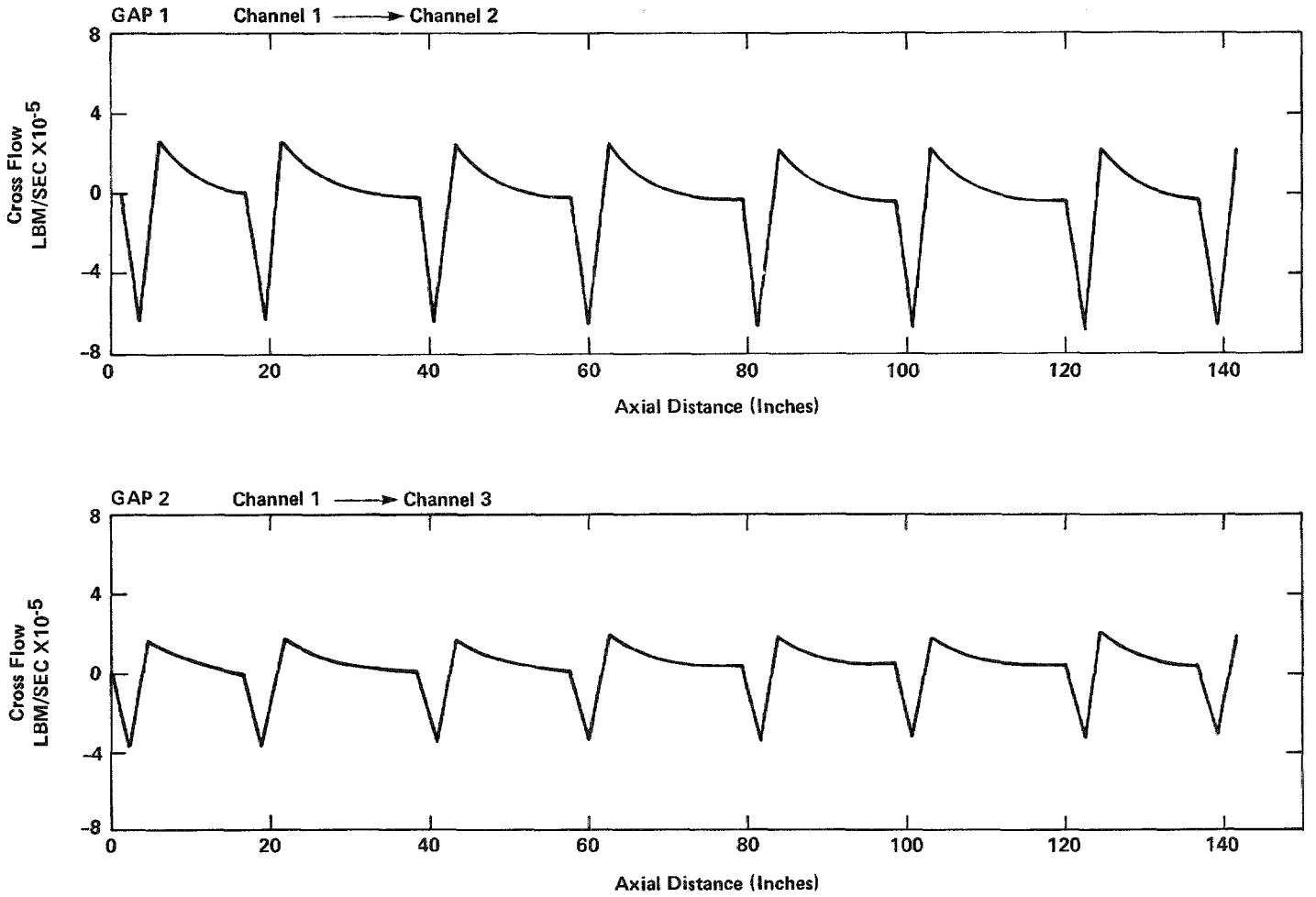

Figure 2-13

Unblocked Bundle Cross Flow Profiles

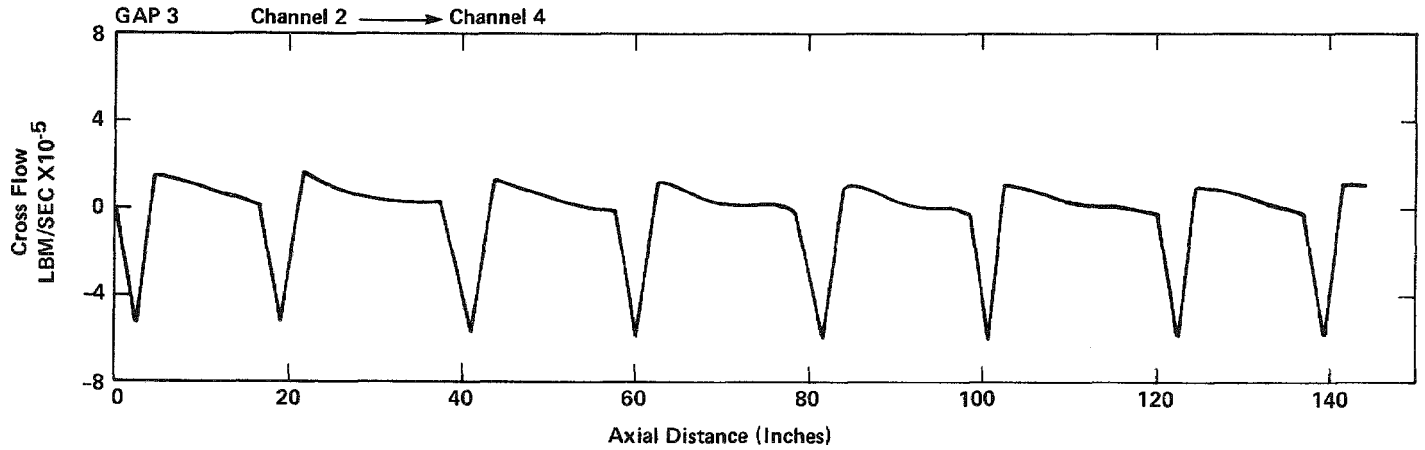

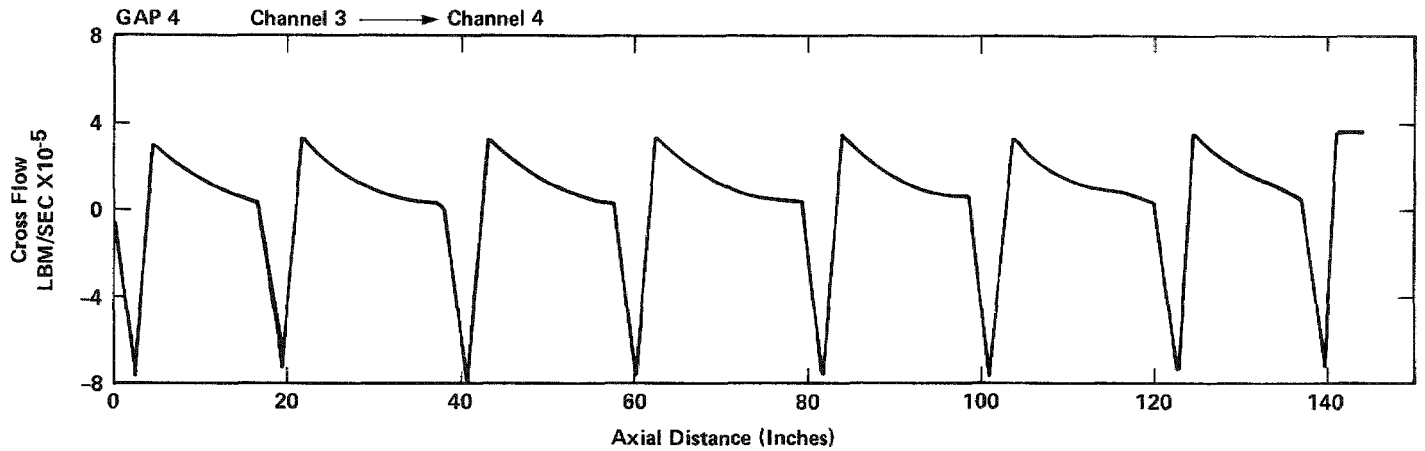

Figure 2-13

Unblocked Bundle Cross Flow Profiles (Cont.)

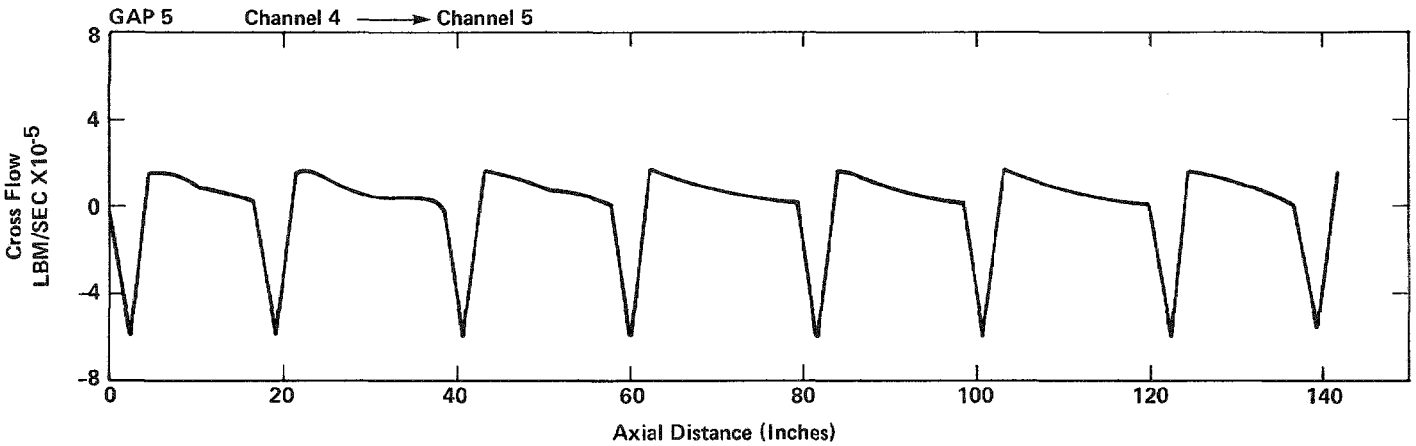

Figure 2-13

Unblocked Bundle Cross Flow Profiles (Cont.)

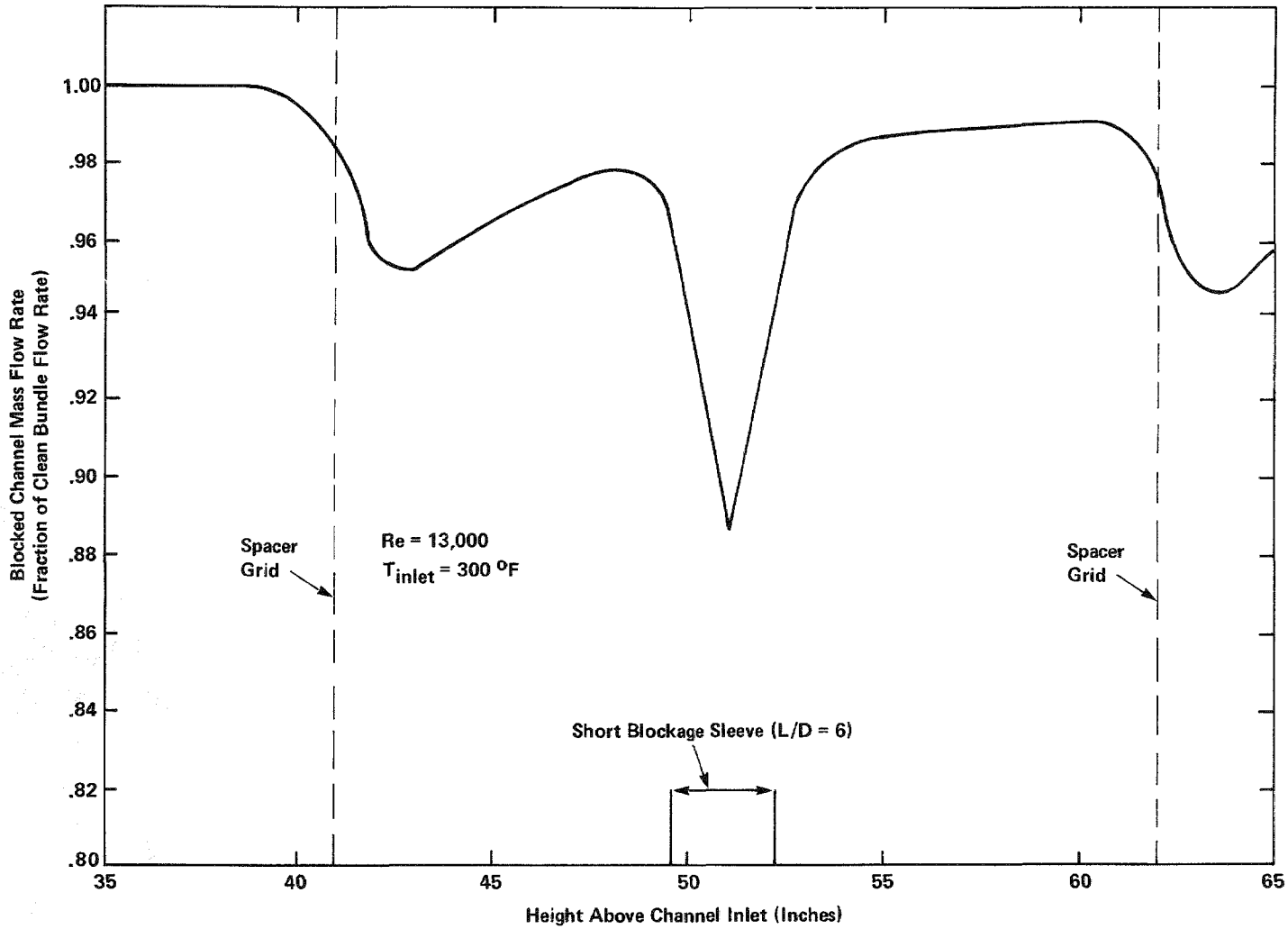

Figure 2-14

Blocked Channel Flow Profile with Spacer Grids

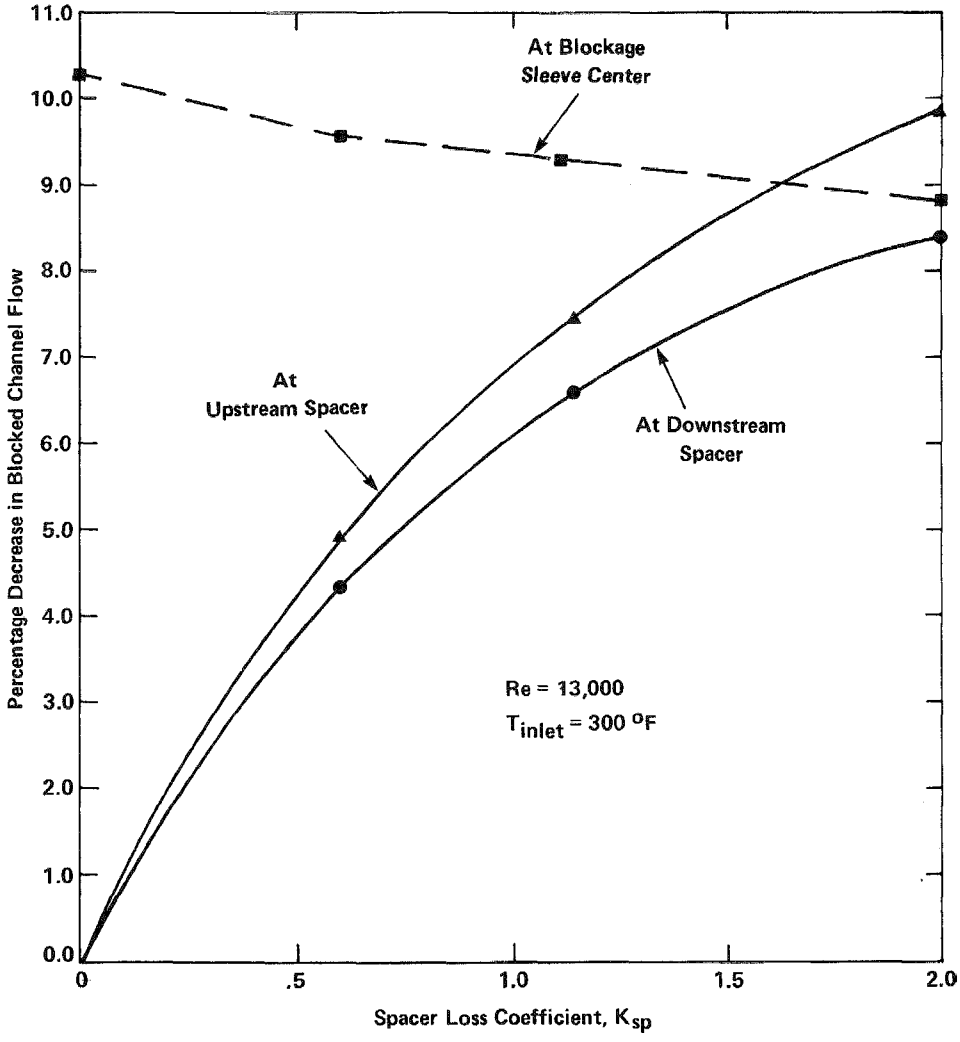

Figure 2-15

Sensitivity of Blocked Channel
Flow to Spacer Loss Coefficient

filler pieces) was preservation of power-to-flow area ratio, which is an important consideration. However, the filler pieces act to depress the mass flux near the periphery, an effect which leads to flow redistribution at the spacers. For the 21-rod bundle, this redistribution affects interior subchannels as shown in Figure 2-14. Spacer grids should, hence, be included in the calculation of local flow velocity distributions in small blocked bundles.

2.5 Thermally Induced Mixing

The analyses discussed in the previous sections were all isothermal, i.e., no heat addition to the fluid from the bundle. In a reflood test, there will be a heat load generated in the bundle and, hence, the steam will be heated as it rises in the bundle. Since the subchannel velocities are unequal, the enthalpy rises will also be unequal. This will induce density differences between subchannels which will promote mixing. This thermally induced mixing is studied by considering the following COBRA steady state simulations: 1) unblocked heated bundle without spacer grids represented; 2) unblocked heated bundle with spacer grids represented; and, 3) single short concentric sleeve blockage in heated bundle with spacer grids represented.

The calculations were performed with the octant model of the 21-rod bundle (see Figure 2-1). In this case the full 144 inch length was modeled. The average heat flux used in the calculation was 3600 Btu/hr-ft^2. The axial heat flux distribution used was the standard 1.66 cosine distribution (see Figure 2-16) specified for the FLECHT-SEASET tests. The combination of assumed average heat flux and 1.66 axial peak results in a peak linear heat generation rate of 0.17 Kw/ft.

2.5.1 Unblocked Heated Bundle Without Spacer Grids

Figures 2-17a through 2-17e show the channel flow profiles for the unblocked heated bundle without spacer grids. Fluid enthalpy versus axial position is shown in Figure 2-18. From this figure it can be observed that thermal mixing acts to equalize the enthalpy in the subchannels. Most of the flow rate changes are small (less than 4%).

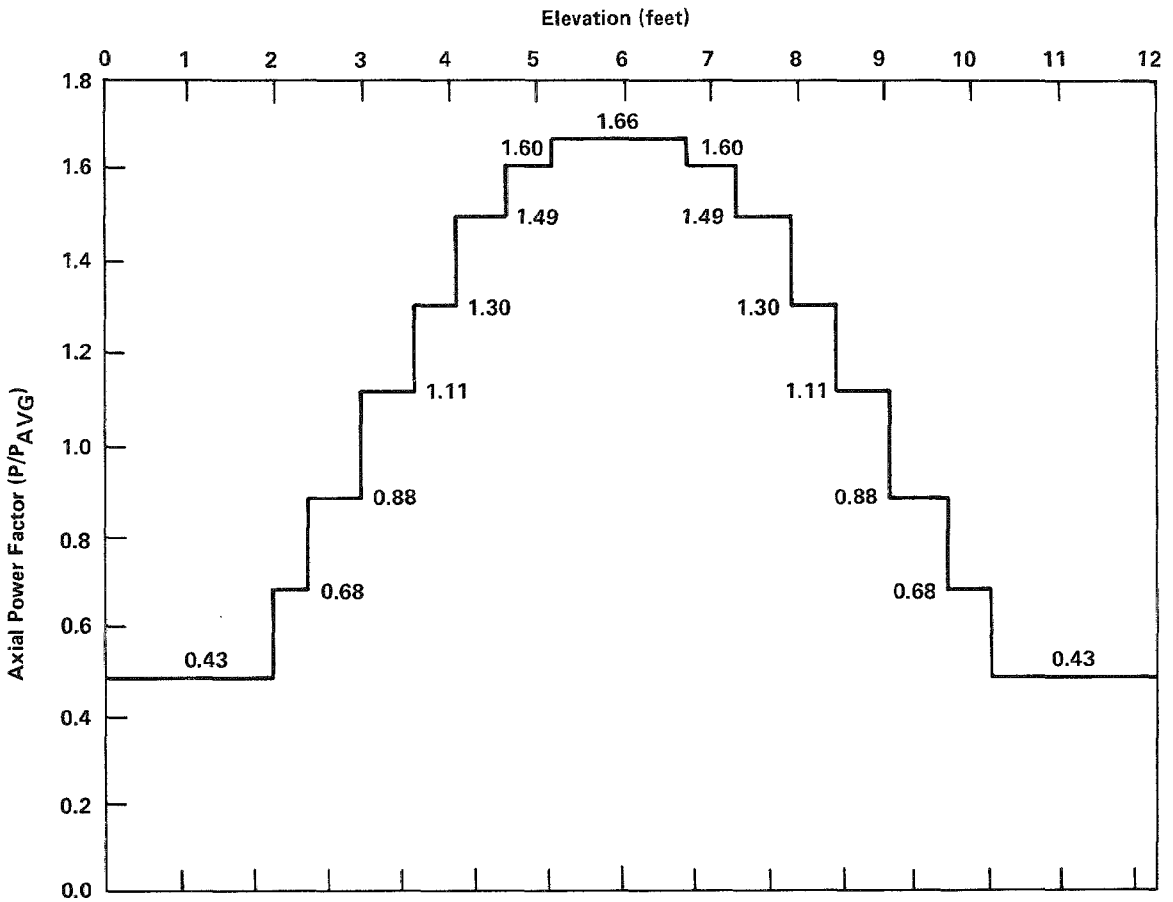

Figure 2-16

FLECHT-SEASET Axial Power Profile

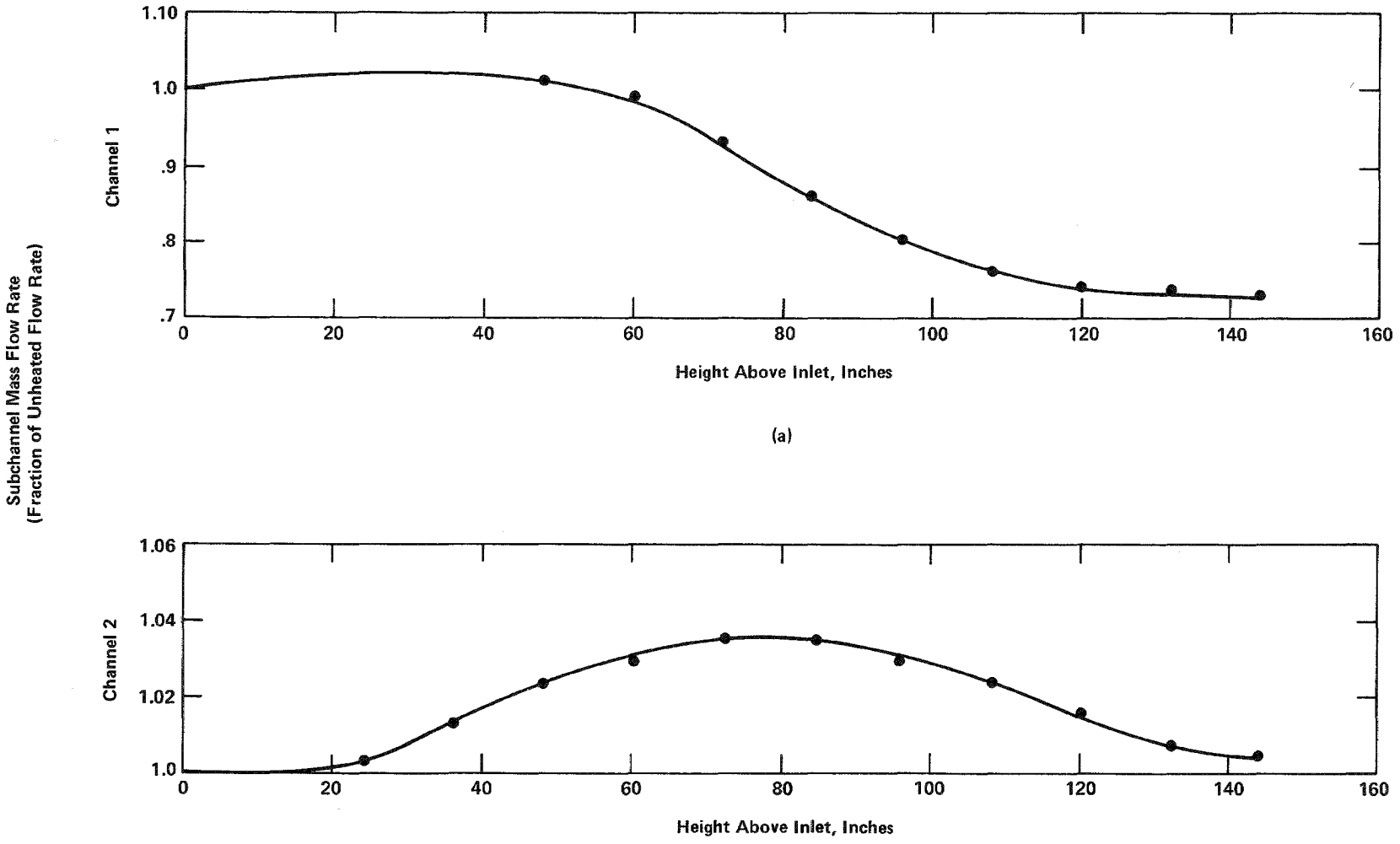

Figure 2-17

Unblocked Bundle Without Spacer Grids Flow Profiles

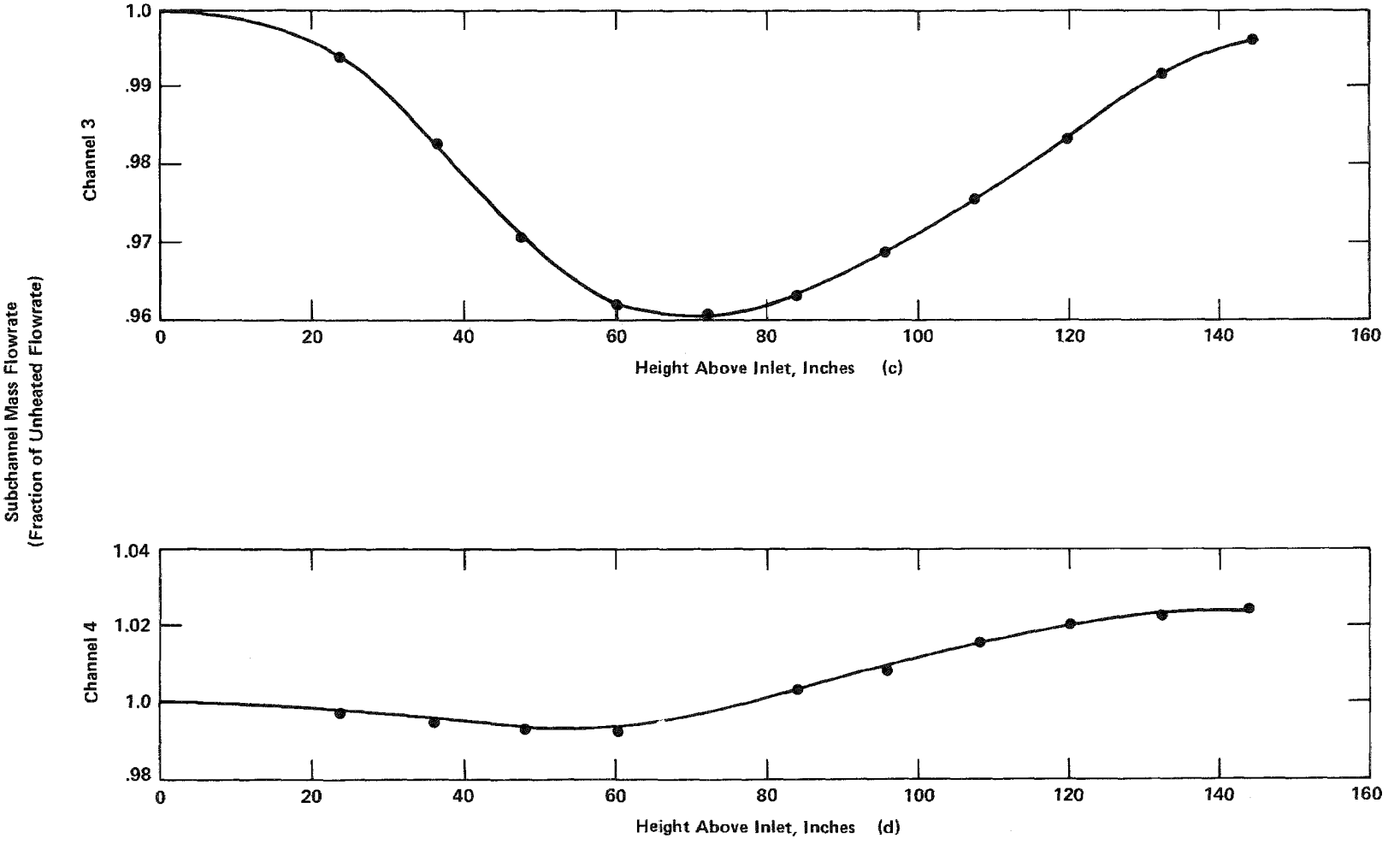

Figure 2-17 (cont.)

Unblocked Bundle Without Spacer Grids - Flow Profiles

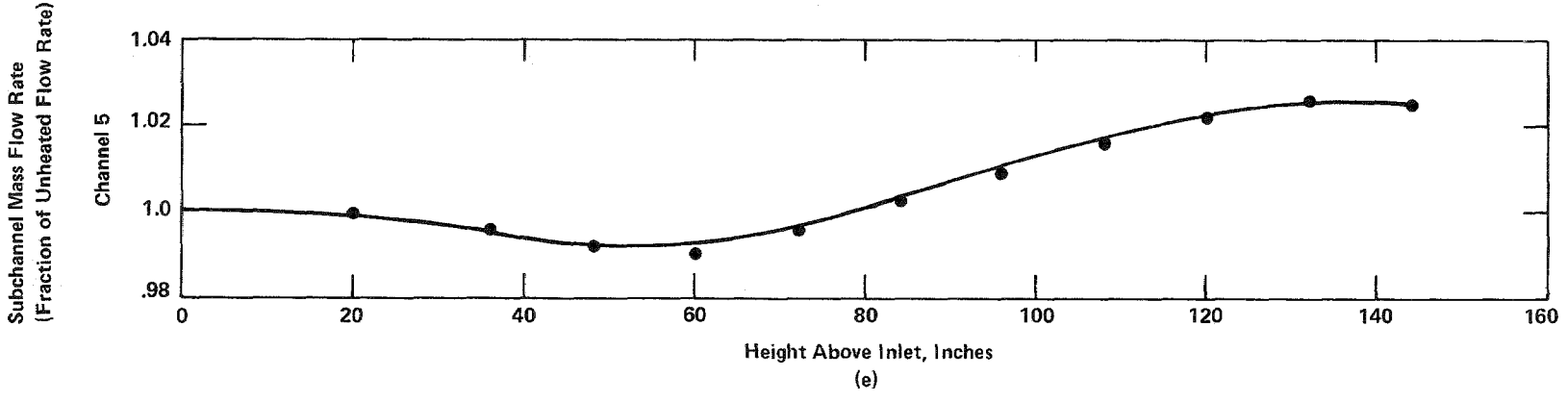

Figure 2-17 (cont.)

Unblocked Bundle Without Spacer Grids - Flow Profiles

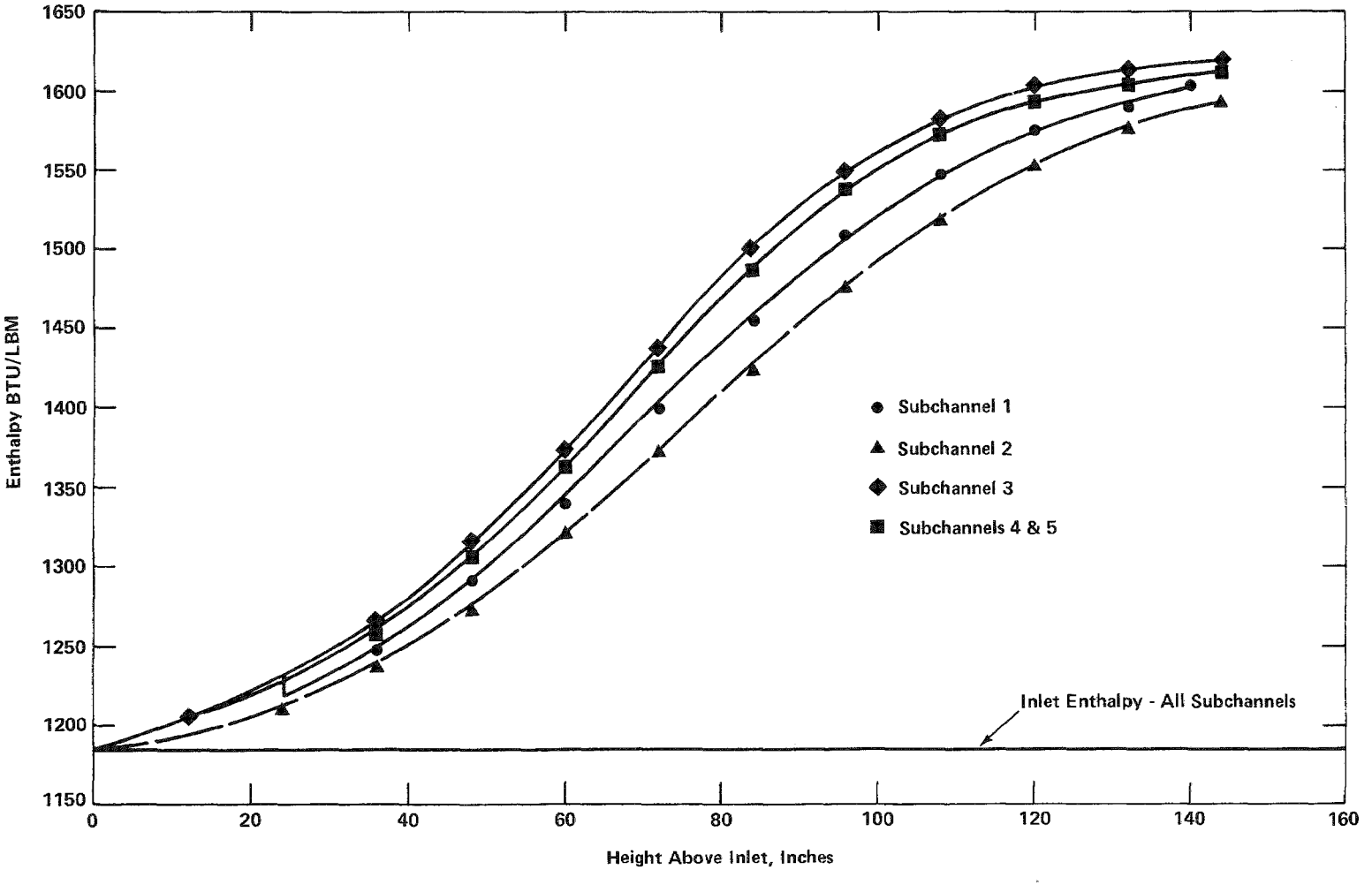

Figure 2-18

Clean Unblocked Bundle Enthalpy Profiles

However, the channel with the smallest hydraulic diameter (Channel 1) has a significant flow reduction on the order of 25%. Therefore, thermal mixing should be considered in calculating local flow conditions in low flow subchannels of a small bundle.

2.5.2 Effects of Spacer Grids

Figure 2-19 shows the flow profile in the central subchannel of the 21 rod bundle (Channel 5) for the case of an unblocked heated bundle with spacer grids represented. The result is essentially a superposition of the "spacer grid oscillation" with the flow profile computed for the heated unblocked bundle without spacer grids. For the purpose of comparison, the channel 5 flow profile for the heated bundle case without spacer grids is also shown in Figure 2-19.

2.5.3 Blocked Channel in Heated Bundle

In Figure 2-20, blocked channel flow profiles are compared for cases with and without heat input to the bundle. The blockage consists of a single short-concentric sleeve on the central rod. The result for the unheated bundle is presented and discussed in Section 2.1.

For the single short concentric sleeve blockage, heating does not appear to have an impact on the level or extent of flow reduction in the blocked channel. Table 2-4 further illustrates this point. The table shows the ratio of the flow in heated and unheated blocked bundle cases to the clean bundle flow. Hence, the results obtained from isothermal calculations should yield appropriate values for the ratio, G_B/G_O.

2.6 Flow Velocity Effects

The sensitivity of the blockage flow redistribution to variation in the bundle average mass flow rate was investigated by performing calculations for various bundle average inlet mass velocities. The calculations were performed for the five rod coplanar blockage in the 21 rod bundle, a situation with large flow diversion. The range of bundle average inlet mass velocity was varied from 0.005×10^6 lb/hr-ft^2 to 0.02×10^6 lb/hr-ft^2.

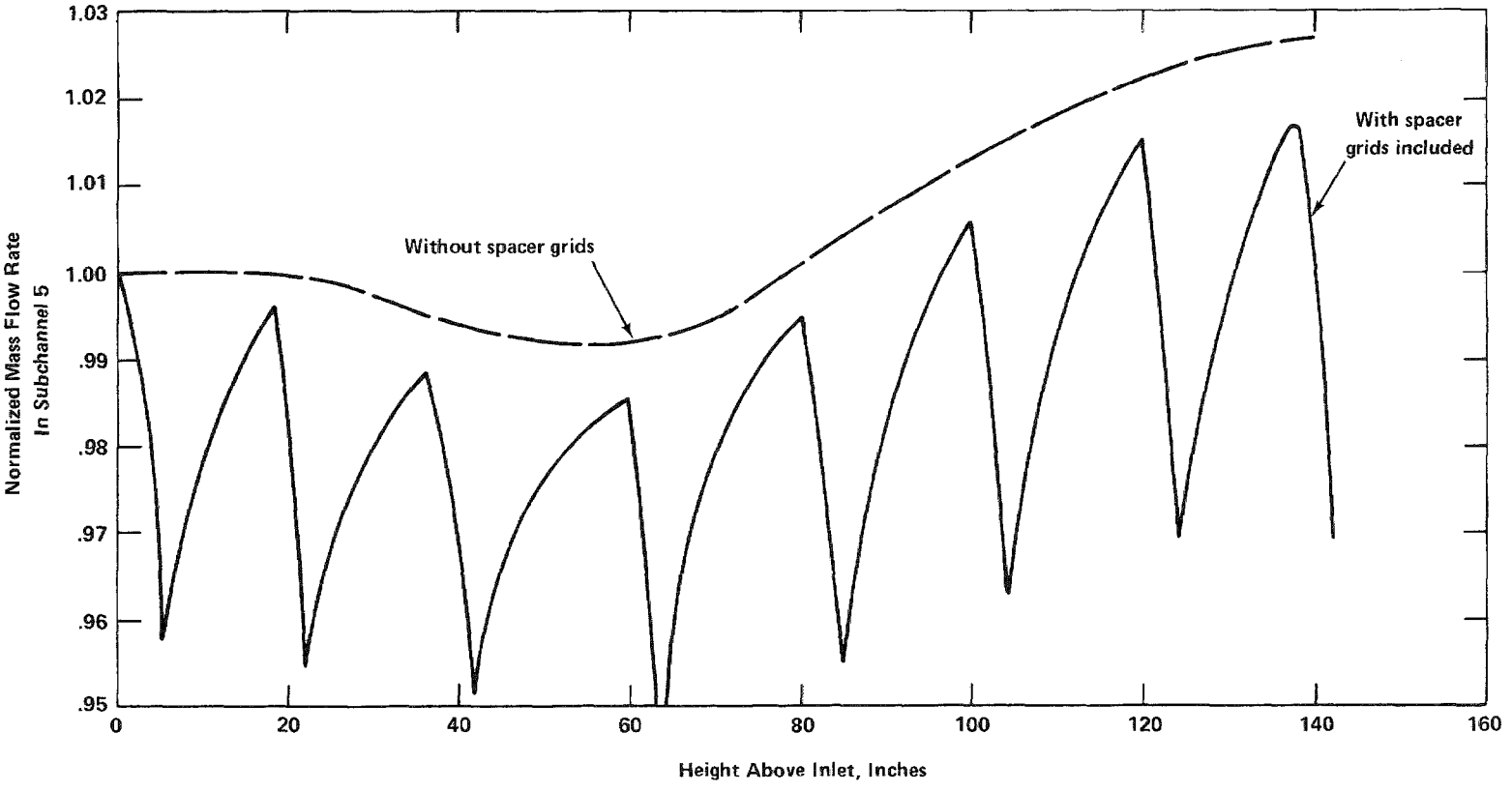

Figure 2-19

Unblocked Heated Bundle Channel Flow Profile

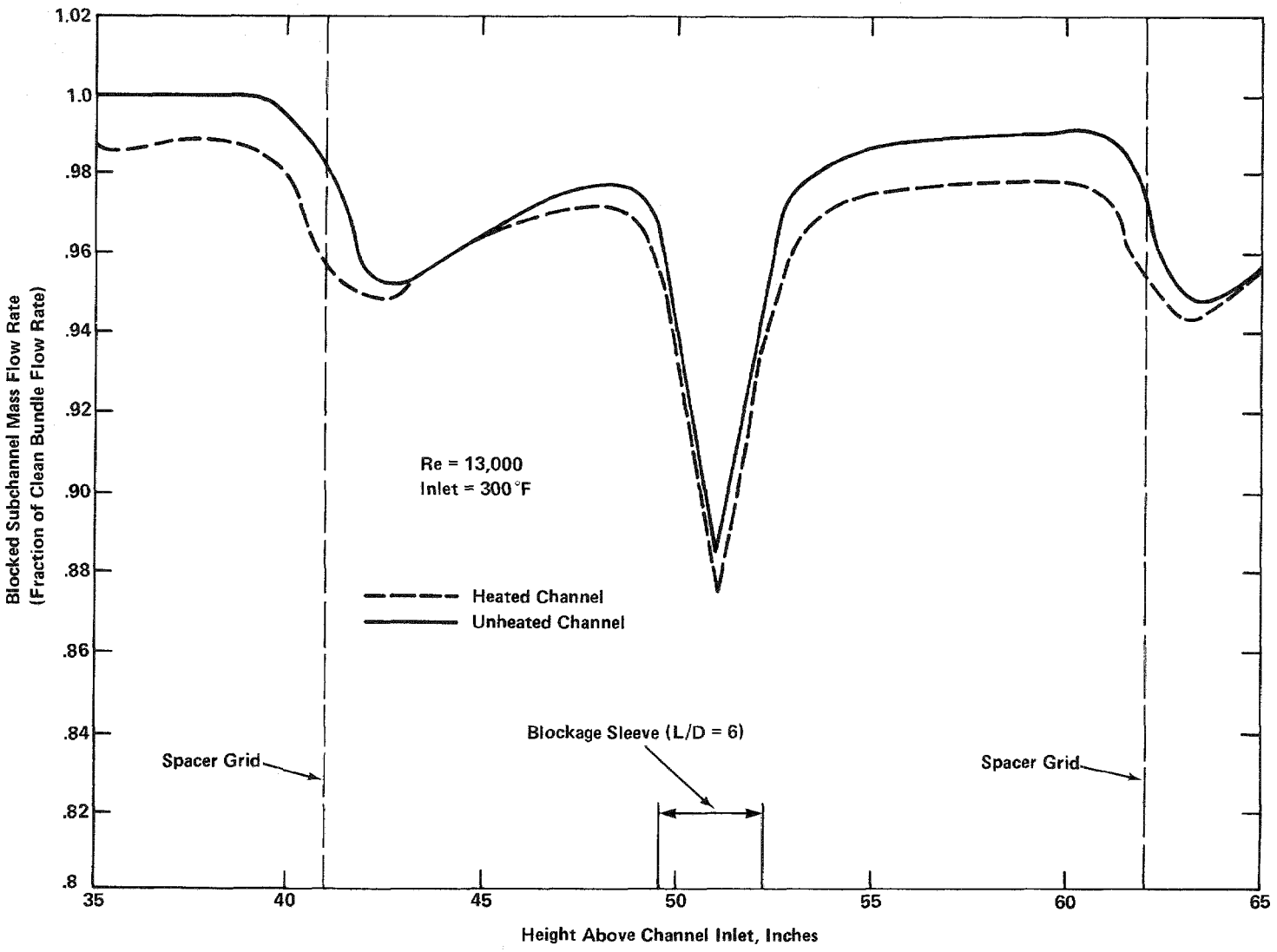

Figure 2-20

Blocked Channel Flow in Heated and Unheated Bundles

A measure of the flow redistribution can be obtained by considering the flow behavior in the subchannel with the largest flow area reduction (subchannel 5 in Figure 2-1). The ratio of the mass velocity at the plane of maximum blockage to the undisturbed mass velocity upstream of the blockage is a measure of the flow redistribution due to the blockage. Table 2-5 gives the values of these mass velocities and the ratios for the three different average inlet velocities. The results indicate that the degree of flow redistribution due to the blockage is insensitive to bundle average inlet mass velocity. Axial flow profiles were also observed to be relatively insensitive to changes in bundle average inlet mass velocity over the range of velocities investigated.

2.7 Comparison with Hochreiter's 21-Rod Bundle Calculations

Comparisons with subchannel calculations from Reference 16 were discussed in Section 2.1 for single blockage sleeves of various lengths on the central rod of the 21-rod bundle. A calculation for coplanar blockage of four adjacent rods with short concentric sleeves was also presented in Reference 16. This same configuration was analyzed using the half bundle COBRA model as shown in Figure 2-21.

Axial flow in the subchannel with the greatest flow restriction (Subchannel 13 in Figure 2-21) is shown in Figure 2-22. Note that the flow diversion is significantly greater than that for a single sleeve blockage. Approximately 60% of the mass flow is diverted from the blocked subchannel. Large cross flows would be expected to occur in the vicinity of the blockage. Figure 2-23 shows the blocked channel axial flow and also the cross flow through one of the four gaps which connect the blocked channel to the rest of the bundle. Note that the magnitude of the cross flow is significant compared to the axial flow. This demonstrates that the cross flow need not be small compared to the axial flow in order to obtain a converged solution with COBRA-IV.

Comparison of the normalized axial flow rate with that computed in Reference 16 shows some differences. Calculations presented in Reference 10 are in closer agreement with those presented here.

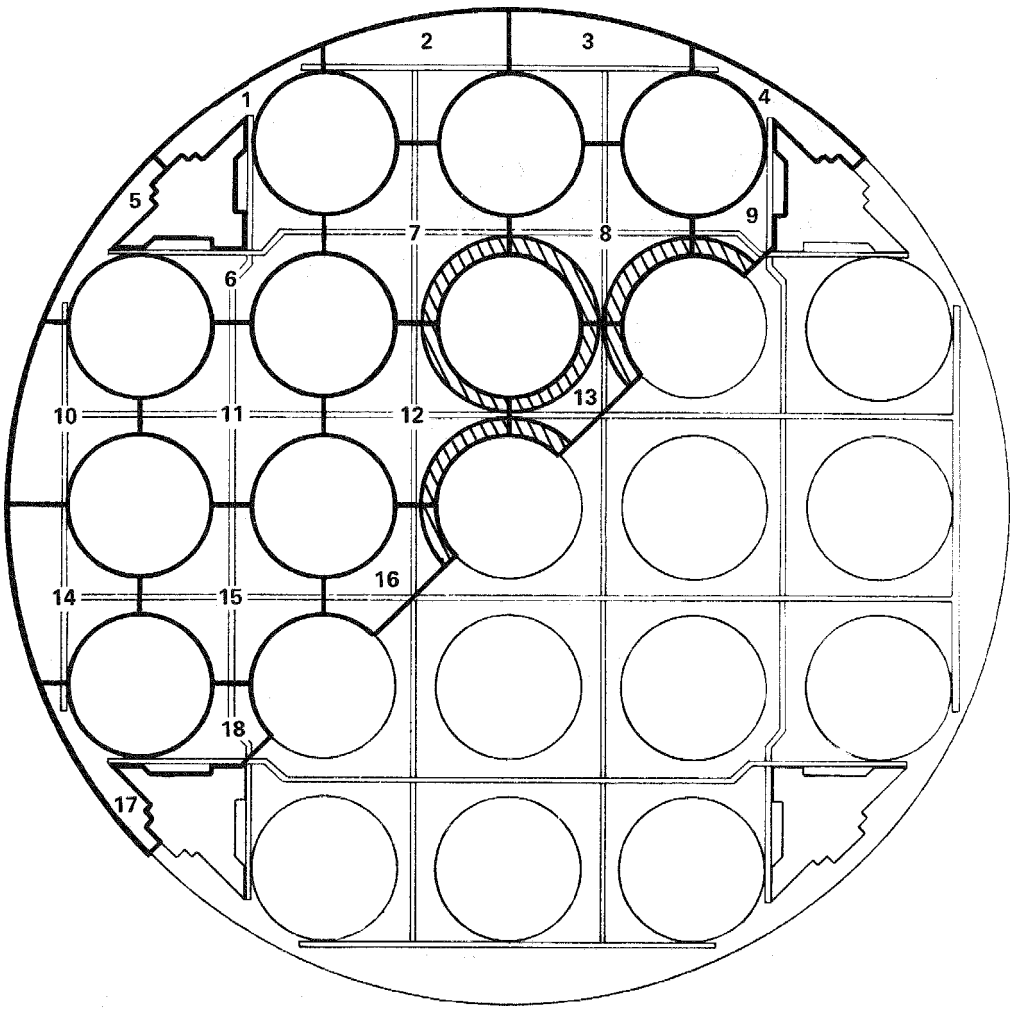

Figure 2-21

Half Bundle Model with Four Rod Blockage

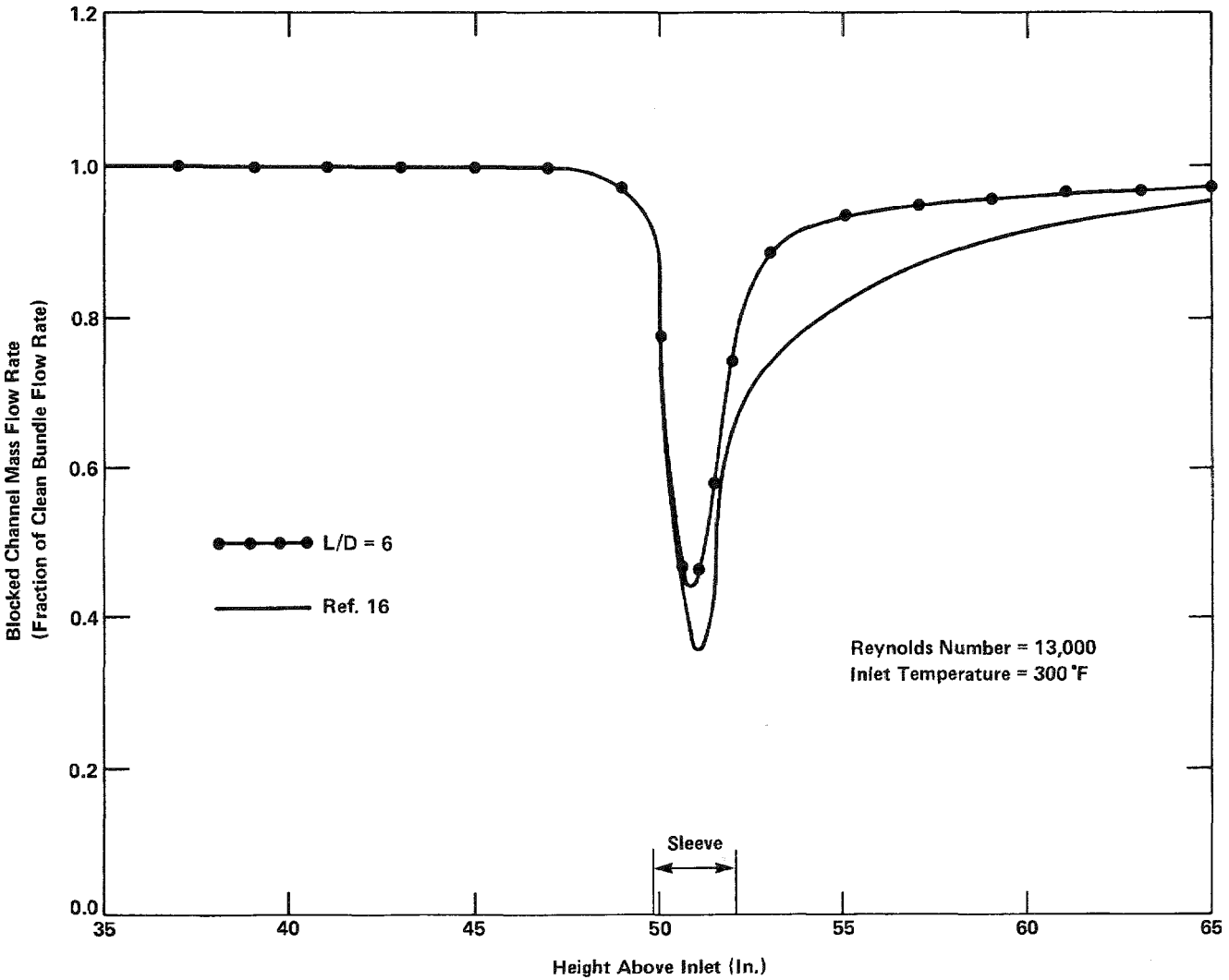

Figure 2-22

Blocked Channel Flow Rate - Four Coplanar Short Sleeves
for Four Rod Blockage in the 21-Rod Bundle

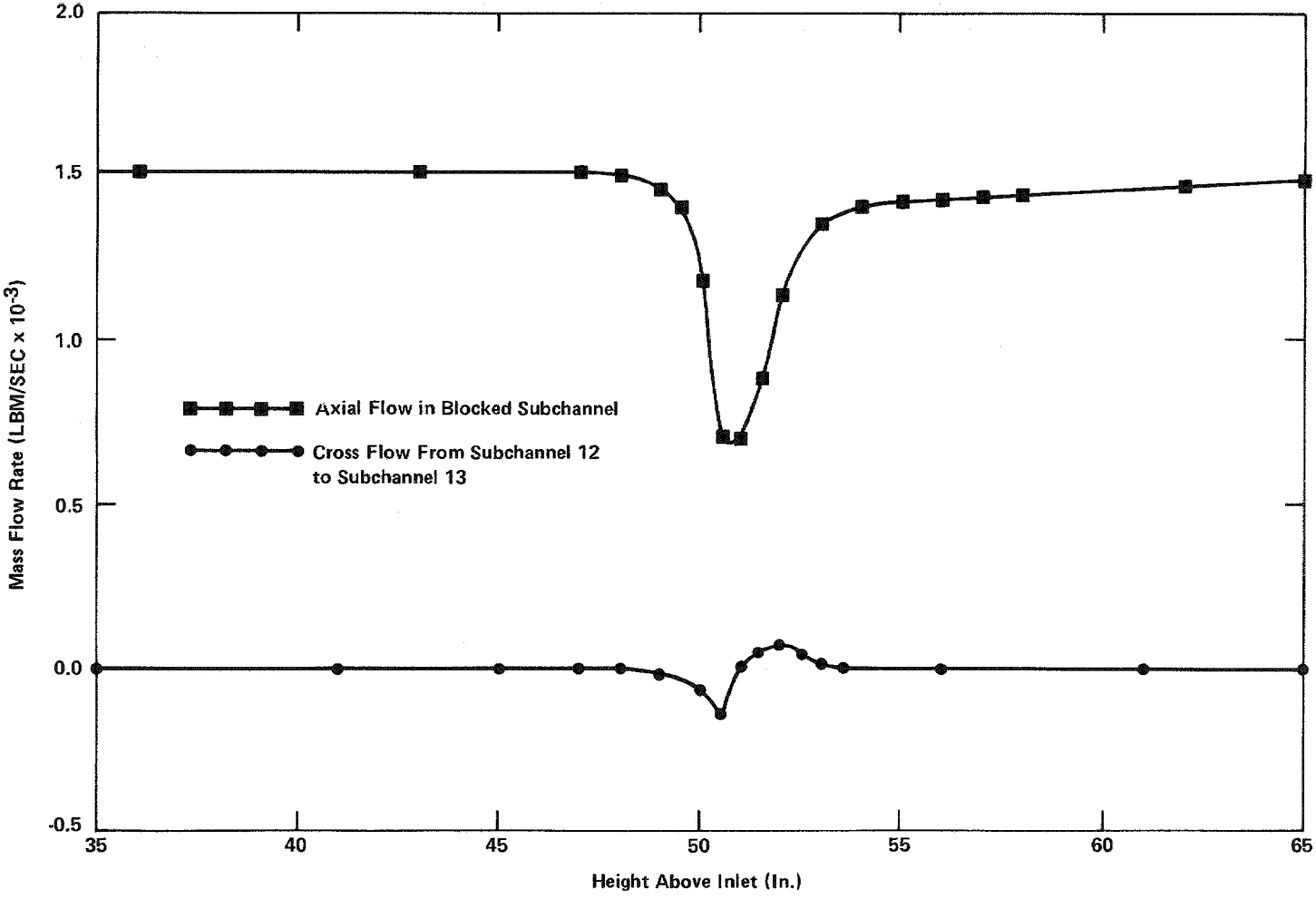

Figure 2-23

Comparison of Axial Flow and Cross Flow
for the Four Rod Blockage

TABLE 2-4

Ratio of Calculated Flow Rate to Clean Bundle

Flow Rate in Maximum Blockage Plane

Subchannel	Heated Bundle Case	Unheated Bundle Case
1	1.038	1.025
2	1.017	1.018
3	1.038	1.030
4	1.028	1.029
5	0.895	0.898

TABLE 2-5

Blocked Channel Flow Dependence

on Bundle Average Mass Flux

Bundle Average Mass Velocity	Local Mass Velocity Upstream of Blockage (G_U)	Local Mass Velocity in Blockage Plane (G_B)	Ratio (G_B/G_U)
(10^6 lb/hr-ft^2)			
0.005	0.00585	0.00527	0.900
0.010	0.0116	0.0105	0.905
0.020	0.231	0.210	0.909

Blank

3.0 FLOW BYPASS CALCULATIONS WITH PLATE BLOCKAGES (JAERI SCTF)

The JAERI slab core test facility consists of eight 16 X 16 electrically heated simulated fuel bundles in a row. A long narrow test vessel encloses the bundles and contains a simulated PWR upper and lower plenum. The test configuration is designed to simulate an axial and radial slice from a typical modern PWR. LOCA reflood tests are conducted in this facility.

COBRA calculations are performed with two (the third and fourth) bundles almost completely blocked at the midplane elevation. This blockage is much more severe than that which has been observed in multi-rod burst tests at ORNL[1] and at Karlsruhe.[2]

The COBRA model for the slab core test facility consists of eight parallel subchannels, one for each 16 X 16 bundle, as shown in Figure 3-1. A large flow area restriction (93%) was used to model the blockage. A full 100% area reduction was not attempted because of anticipated numerical problems. The 93% blockage was the only case run.

Important parameters in the COBRA model are listed in Table 3-1. The mass flux is the final bundle average value reached after a linear ramp increase over one-half second. Final steady state flow is superheated steam at 400° F and a Reynolds number of 4100. A total of 60 axial nodes are used in each channel for a node length of 2.4 inches. The blockage is all concentrated in the single axial node beginning at elevation 72 inches in Channels 3 and 4. Blockage loss coefficients were used only in subchannels with blockages, as in Reference 7. Values for the loss coefficients were estimated using formulae in Reference 17. For plate blockages, form losses have been found to be significant and, therefore, they were included in the model.

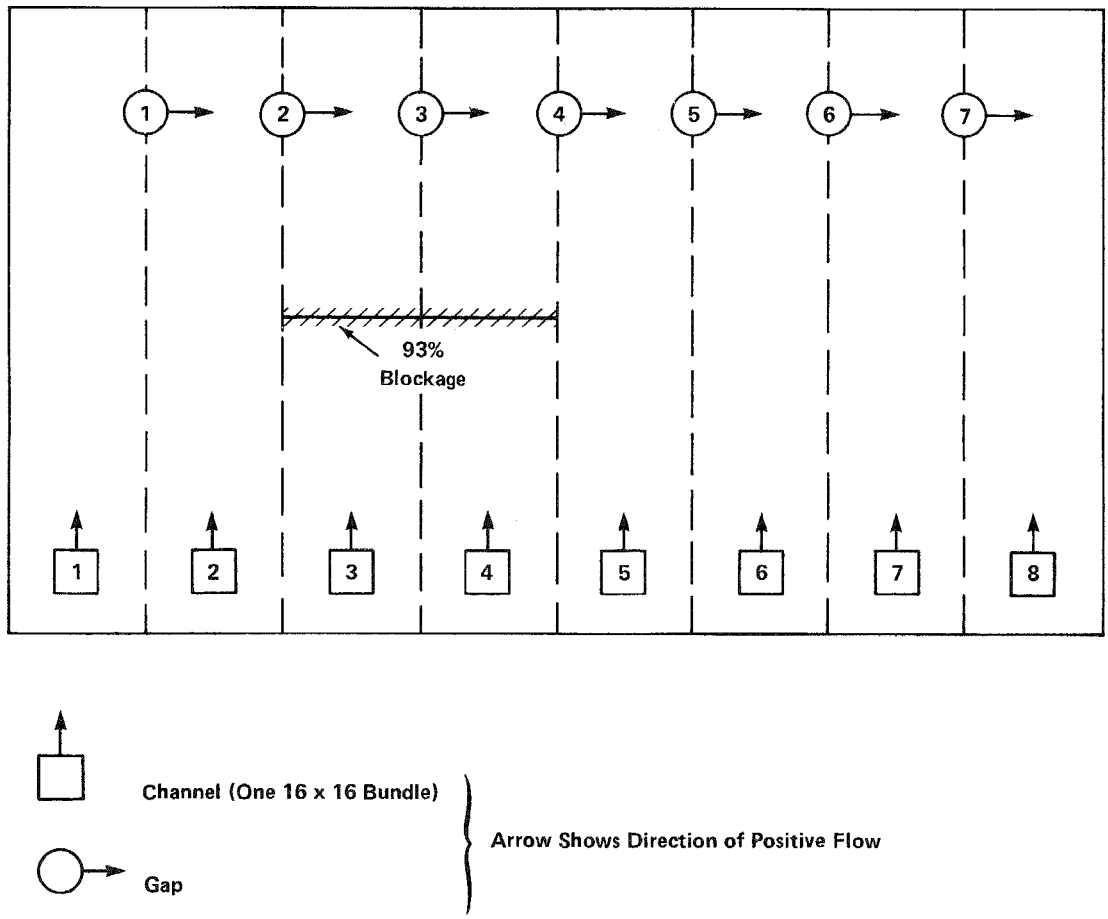

Figure 3-1

Schematic of SCTF COBRA Model

TABLE 3-1

Key Parameters in SCTF COBRA Model

Heater Rod Diameter	10.7 mm (0.42 in.)
Non-heater Rod Diameter	13.8 mm (0.54 in.)
Heater Rods/Bundle	234
Non-heater Rods/Bundle	22
Rod Pitch	14.3 mm (0.56 in.)
Bundle Pitch	230 mm (9.05 in.)
Heated Length	3660 mm (144 in.)
Pressure	5.784 atmospheres (85 psia)
Mass Flux	5.425×10^{-7} kg/m^2- sec (4000 lb/hr-ft^2)
Temperature	$204^{\circ}C$ ($400^{\circ}F$)
Lateral Resistance Factor	5.0
s/l Parameter (Gap Spacing/Gap Length)	0.2558
Turbulent Momentum Factor	1.0
Bare Rod Friction Factor	$0.316\ Re^{-0.25}$
Subchannel Blockage Loss Coefficient	
Channels 3,4	25.0
Chanels 1, 2, 5, 6, 7, 8	0.0
Turbulent Mixing Parameter	0.02

To arrive at a converged solution for this blockage case, it was necessary to obtain the asymptotic steady state result of a transient case. The run was initiated with zero flow in the bundle. A ramp increase to the full steady state inlet flow was applied as a time dependent boundary condition. In this way, the cross flows were always close to the solution since values from the last time step are used as a first guess at the present time step. When a steady state calculation is attempted, the cross flows are found iteratively by starting with zero cross flow as the initial guess. In many cases, a converged solution for the cross flows cannot be obtained using the normal steady state technique. This is especially true for large blockages where the magnitude of the cross flow is large.

Figures 3-2 and 3-3 show the normalized axial flow plotted as a function of axial distance. Note that there is a large decrease in flow to approximately 5% of the bundle average flow at the blockage location. Large regions with low flow extend both upstream and downstream of the blockage. Note that the flow increases substantially in the unblocked channels adjacent to the blockage. The prediction of a large low flow region is consistent with results of experiments conducted for large sleeve blockages.[6,7] In these experiments, a 90% subchannel blockage resulted in a recirculation region extending up to five hydraulic diameters downstream of the blockage. In a region of very low flow downstream of the blockage, overheating might possibly occur. Since this type of plate blockage has not been observed in rod burst tests, it would appear to be more desirable to test sleeve blockages.

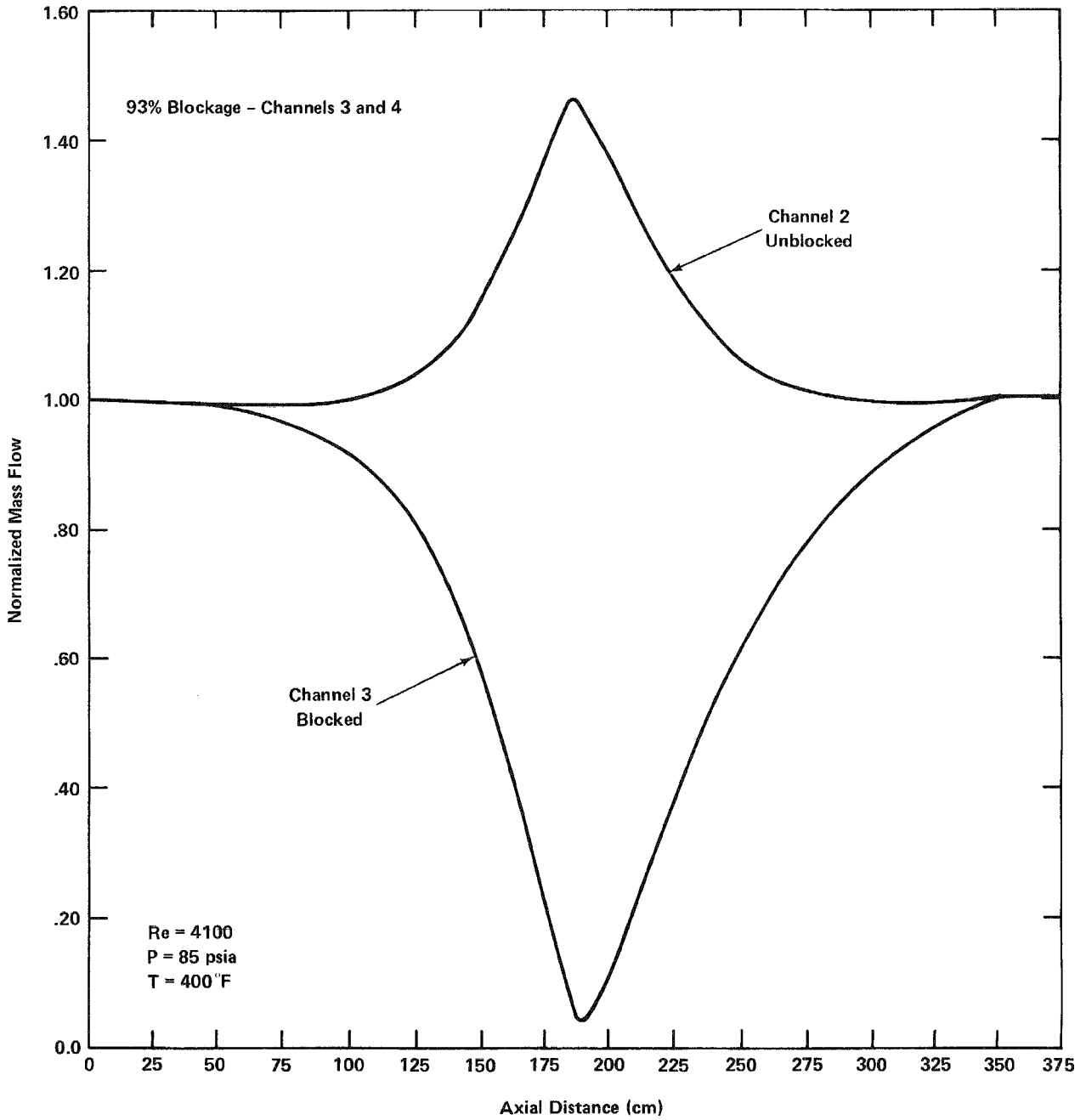

Figure 3-2

Flow in Blocked and Unblocked Channels 3 and 2

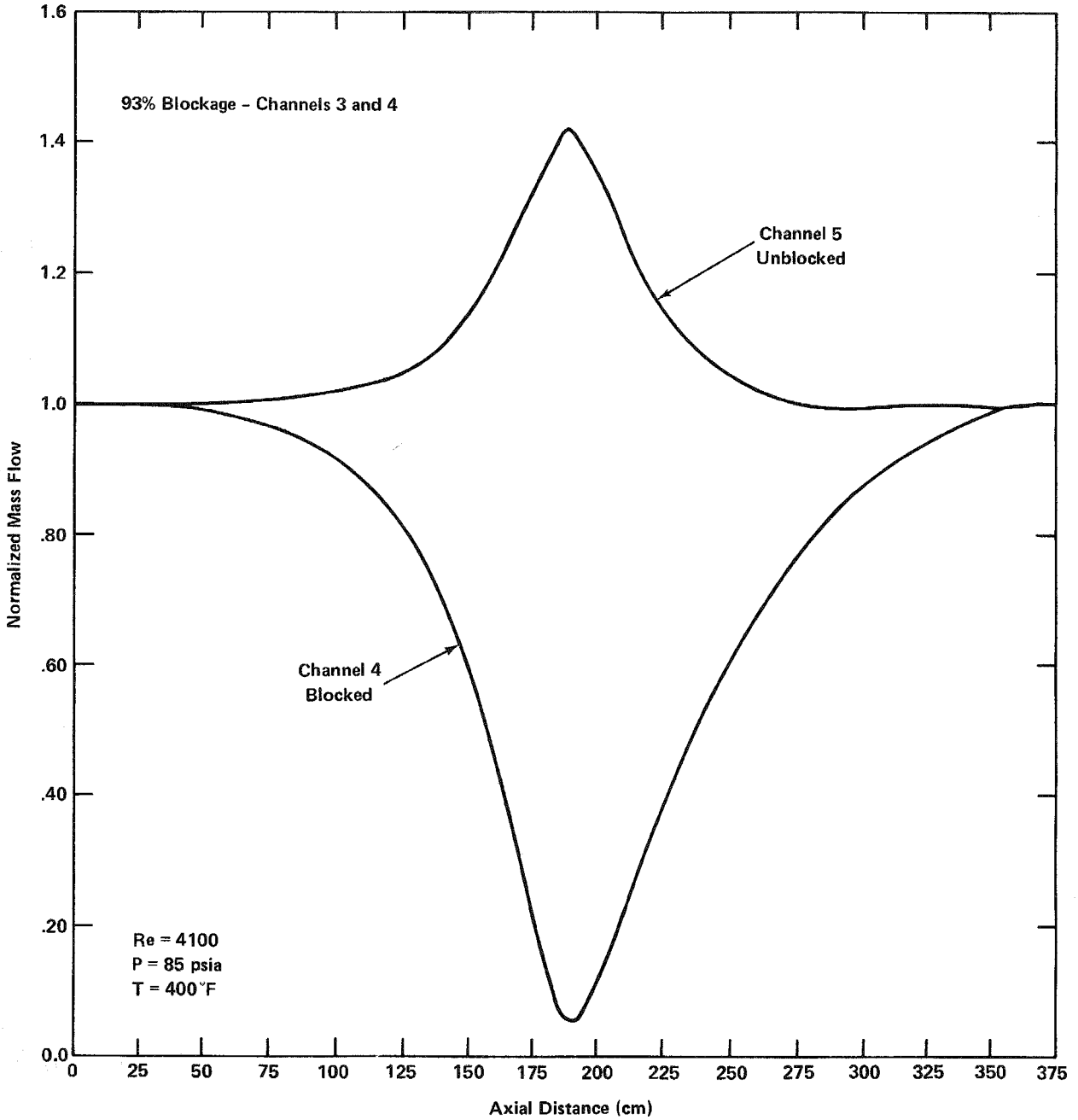

Figure 3-3

Flow in Blocked and Unblocked Channels 4 and 5

4.0 PRESSURE DROP DUE TO BLOCKAGE

Figures 4-1 and 4-2 show pressure drop along the FLECHT-SEASET 21-rod bundle length as calculated by COBRA for the five rods blocked and all rods blocked cases (Section 2.3), respectively. Spacers were not included in these calculations. The blockages were modeled as area variations with no additional form loss coefficients.

The pressure drop per unit length of the rod bundle is constant in the absence of blockages. The dashed lines in Figures 4-1 and 4-2 show what the pressure drops would be in the absence of blockages, i.e., for a clean bundle. The additional irrecoverable losses due to the blockage are denoted as ΔP_{Block}.

Figure 4-3 shows the pressure drop in the vicinity of the single short concentric blockage sleeve in the FLECHT-SEASET 21-rod bundle. This simulation also includes spacer grids which were not included in the two cases discussed above. Note that the irrecoverable pressure drop due to the blockage is negligible.

Mincey[14] compared COBRA calculated pressure drop for blocked bundles with experimental data over a range of Reynolds numbers. The area variation alone was found to be sufficient to reproduce the data, provided that a suitable friction factor correlation was used. However, Mincey's data comparisons with the reference (unblocked) bundle seem to indicate that the friction factor used is too high. Use of the higher friction factor was justified on the basis of a pitch to diameter ratio dependence reported in Reference 18.

Rowe *et al.*,[4] used both area variation and an additional form loss in the blocked channels to model sleeve and plate blockage pressure losses. The additional form loss coefficients were determined from measured pressure drop data. Sleeve blockages typically gave

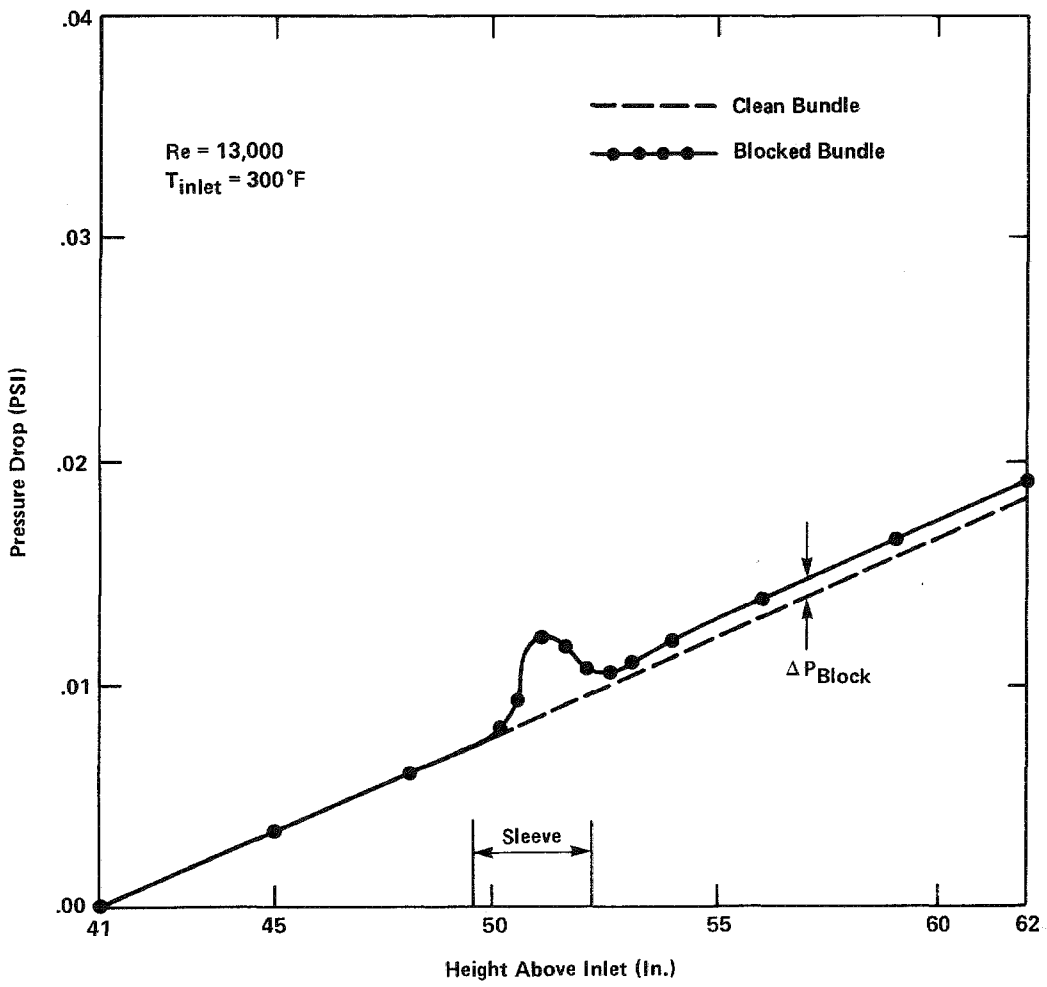

Figure 4-1

Pressure Drop for Five Rod Blockage in the
FLECHT-SEASET 21-Rod Bundle

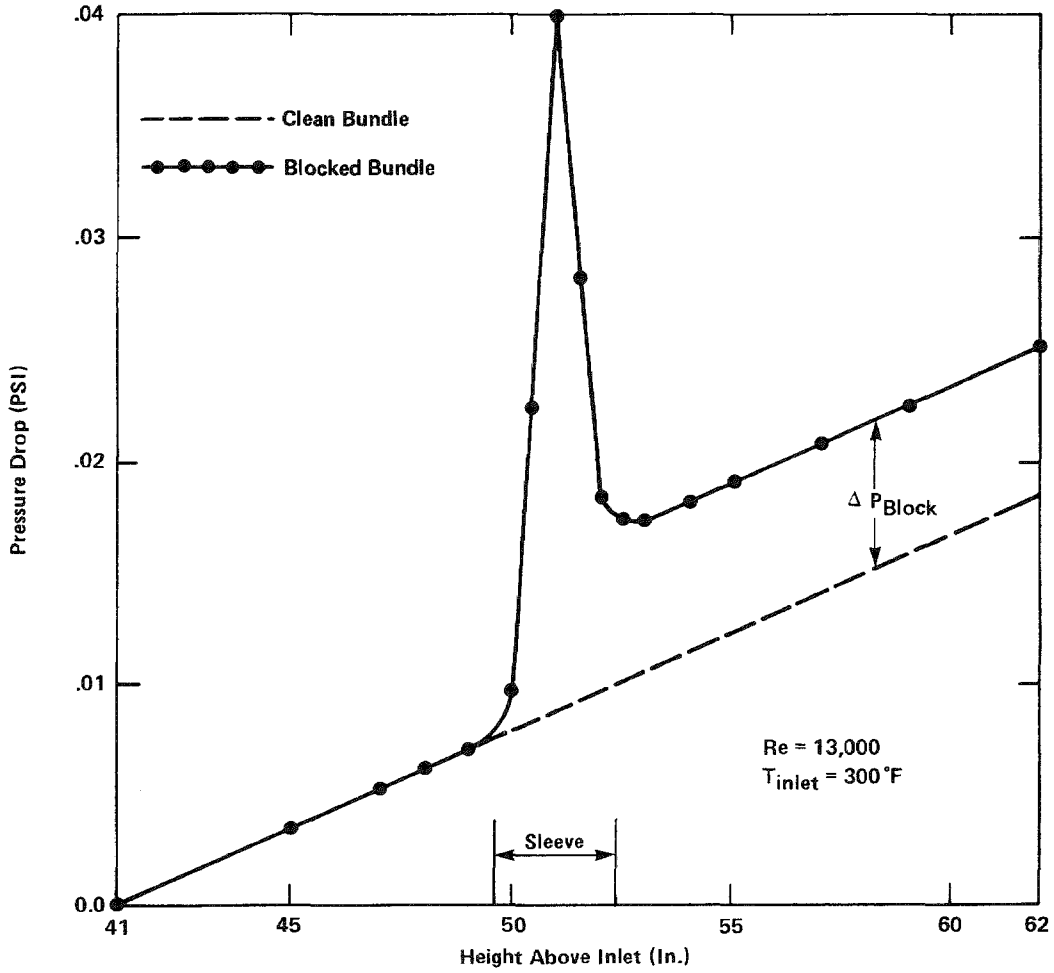

Figure 4-2

Pressure Drop for All Rods Blocked in the FLECHT-SEASET 21-Rod Bundle

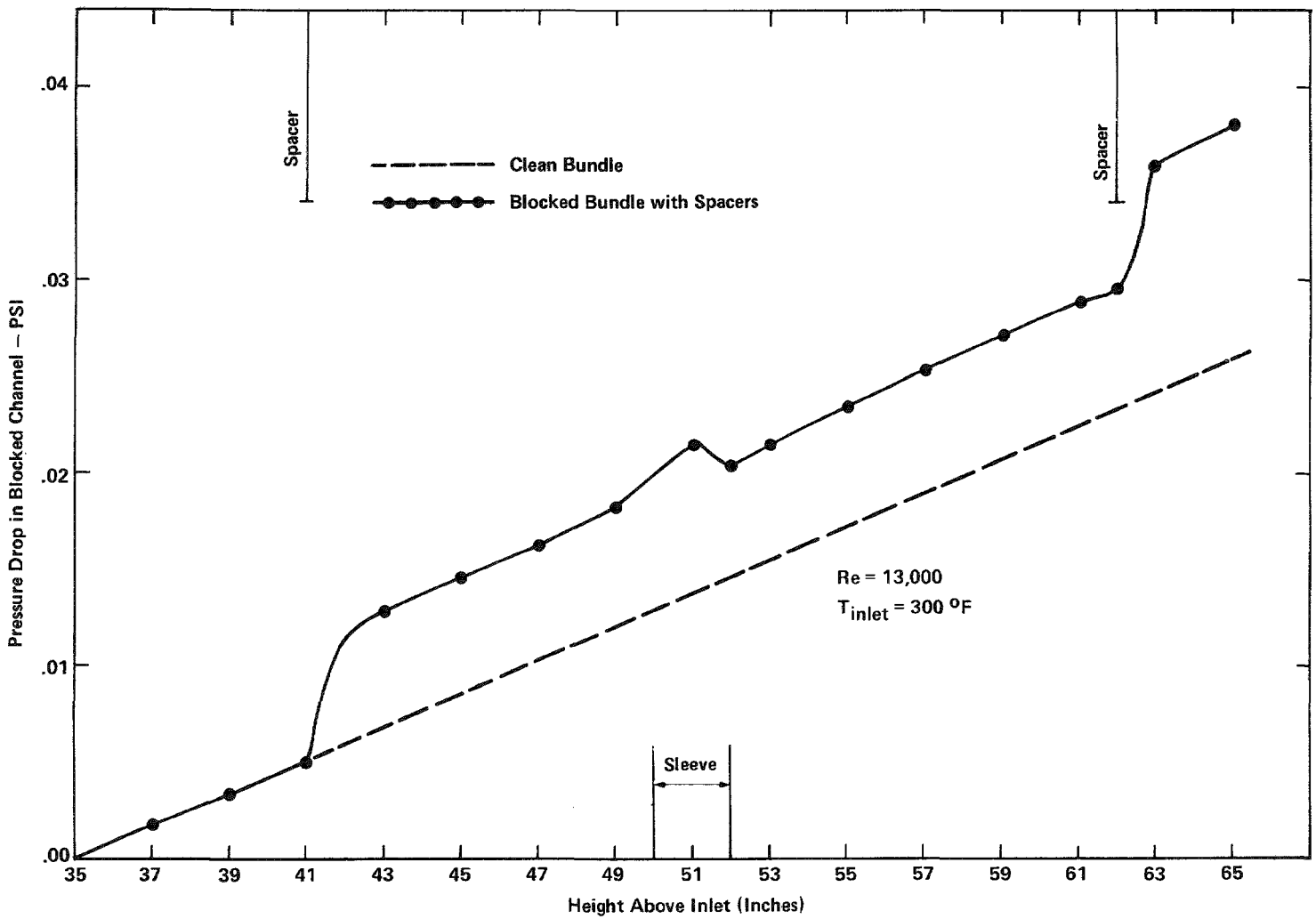

Figure 4-3

Pressure Drop for Single Sleeve Blockage in FLECHT-SEASET 21-Rod Bundle

additional loss coefficients which were small compared to those of plate blockages. Since the FLECHT-SEASET blockage sleeves are smaller than those used by Rowe, additional blockage form losses were assumed to be insignificant. Hence, pre-test predictions of blockage pressure losses for bundle hydraulic tests can be made using the models developed here (with test flow conditions). If necessary, the results can be corrected by addition of form losses.

It is noted that, according to Reference 4, "The area reduction model is the major mechanism of providing forced flow diversion from the blocked subchannels and the primary purpose of the blockage loss coefficients is to account for the irrecoverable form pressure loss." Therefore, the results presented in previous sections which model blockages as flow area reductions are valid for determining flow redistribution.

5.0 CONCLUSIONS

Based on the variety of blockage configurations simulated, it is concluded that COBRA-IV-I is capable of calculating flow redistribution caused by blockages, including cases with relatively large crossflow. It does not appear to be desirable to use either the gap spacing variation model or the lateral momentum flux option in COBRA-IV-I. Calculated results proved to be insensitive to these options which sometimes caused numerical difficulties.

Following are the significant observations which have been made as a part of this study:

1. Spacer grids in a small bundle can cause flow redistribution comparable to that of sleeve blockages. Therefore, spacer grid effects should be included when calculating local velocity for input to mechanistic models of blocked bundle heat transfer.

2. Subchannel flow redistribution does not appear to be a strong function of bundle average velocity. Therefore, the ratio of blocked subchannel flow to clean bundle subchannel flow will not vary significantly with average bundle velocity. Since this ratio is to be used in mechanistic models in the FLECHT-SEASET program, the ratio need only be calculated for a relatively few flow rates.

3. Preliminary calculations [16] of flow redistribution in the FLECHT-SEASET 21 rod bundle were found to contain an anomalous flow overshoot downstream of the blockage. Subsequent calculations [10] do not exhibit this anomalous behavior.

4. Axial flow at the plane of maximum blockage is not sensitive to the inclusion of low strain "tails" on a blockage sleeve. This confirms the conclusion of Reference 16.

5. Thermally induced mixing which occurs in a heated bundle may change the flow in subchannels near the periphery of a bundle compared to the isothermal case. However, for interior channels, the ratio of blocked channel flow to clean bundle flow is not significantly affected by thermally induced mixing.

6. A single FLECHT-SEASET long non-concentric sleeve will give greater flow diversion than a single short concentric sleeve. Also, the flow will vary around the periphery of the long non-concentric sleeve.

7. The largest flow diversion will occur for a cluster blockage rather than for a total (i.e., sleeves on all rods) bundle blockage. This was demonstrated by a comparison of a total bundle blockage with a five rod blockage in the FLECHT-SEASET 21-rod bundle.

8. Pressure drop can be calculated for various sleeve blockage configurations based only on the flow area reduction resulting from the blockage. Validation of this method awaits data from the FLECHT-SEASET 21-rod bundle task.

9. A complete plate blockage of two of eight assemblies in the JAERI SCTF will result in very low flow both upstream and downstream of the blockage. This blockage is not typical of that observed in rod bundle burst tests.

6.0 REFERENCES

1. R. H. Chapman, ORNL Multi-Rod Burst Tests - Recent Results, Current Status, and Future Plans, presented at Zircaloy Cladding Research Review Meeting, Idaho Falls, Idaho, June 25, 1979.

2. E. H. Karb, "In-Pile Tests at Karlsruhe of LWR Fuel-Rod Behavior During the Heatup Phase of a LOCA, Nuclear Safety, Vol. 21, No. 1, January-February 1980.

3. F. Erbacher, et al., Studies on Zircaloy Fuel Clad Ballooning in a LOCA, Results of Burst Tests with Indirectly Heated Fuel Rod Simulators, presented at the ASTM Fourth International Conference on Zirconium in the Nuclear Industry, Stratford-on-Avon, England, June 27-29, 1978.

4. D. S. Rowe, et al., "An Experimental Study of Flow and Pressure in Rod Bundle Subchannels Containing Blockages," BNWL-1771, September 1973.

5. D. S. Rowe, "COBRA-IIIC: A Digital Computer Program For Steady State and Transient Thermal Hydraulic Analysis of Rod Bundle Nuclear Fuel Elements," BNWL-1695, March 1973.

6. J. M. Creer, et al., "Effects of Sleeve Blockages on Axial Velocity and Intensity of Turbulence in an Unheated 7 X 7 Rod Bundle, BNWL-1965, January 1976.

7. J. M. Creer and J. M. Bates, "Effects of Sleeve Blockages on Air Velocity Distributions in an Unheated 7 X 7 Rod Bundle," BNWL-1975, January 1976.

8. J. M. Creer et al., "Turbulent Flow in a Model Nuclear Fuel Rod Bundle Containing Partial Flow Blockages," Nuclear Engineering and Design, No. 52, 1979, pp. 15-33.

9. C. E. Conway, et al., PWR FLECHT Separate Effects and Systems Effects Test (SEASET) Program Plan, NRC/EPRI/Westinghouse Report No. 1, December 1977.

10. L. E. Hochreiter, et al., PWR FLECHT-SEASET 21-Rod Bundle Flow Blockage Task: Task Plan Report, NRC/EPRI/Westinghouse Report No. 5, NUREG/CR-1370, NP-1382, WCAP-9658, March 1980.

11. C. L. Wheeler, et al., "COBRA-IV-I: An Interim Version of COBRA for Thermal-Hydraulic Analysis of Rod Bundle Nuclear Fuel Elements and Cores," BNWL-1962, March 1976.

12. C. W. Stewart, et al., "Core Thermal Model: COBRA-IV Development and Applications," BNWL-2212, January 1977.

13. C. W. Stewart, et al., "COBRA IV: The Model and The Method," BNWL-2214, July 1977.

14. J. F. Mincey, MRBT Flow Tests at ORNL: A Determination of Bundle Pressure Losses Along the Axis, presented at the Quarterly Cladding Review Meeting, Oak Ridge National Laboratory, April 25-26, 1978.

15. K. Rehme, "Pressure Drop Correlations for Fuel Element Spacers," Nuclear Technology, Vol. 17, January 1973, pp. 15-23.

16. L. E. Hochreiter, et al., PWR FLECHT-SEASET 21-Rod Bundle Flow Blockage Task: Task Plan Report, NRC/EPRI/Westinghouse Report No. 4 (DRAFT), November 1978.

17. I. E. Idel'chik, Handbook of Hydraulic Resistance Coefficients of Local Resistance and of Friction, AEC-TR-6630, 1966.

18. L. S. Tong, "Pressure Drop Performance of a Rod Bundle", in Heat Transfer in Rod Bundles, papers presented at the ASME Winter Annual Meeting, New York, N. Y., December 3, 1968.